Modelling of fracture by cohesive force models: a path to pursue

Jean-Jacques Marigo

Sorbonne Université, 4 place Jussieu, Paris 75005, France

ARTICLE INFO

Keywords:
Cohesive forces
Strength of materials
Fracture
Fatigue
Variational approach
Two-scale approach

ABSTRACT

Phase field models have been very successful in recent years and tend to become hegemonic in modelling the fracture of materials. This is primarily due to their ease of implementation to account for the entire fracture process including nucleation and propagation of cracks. In doing so, the cohesive force models have been somewhat neglected although they are based on better established physical bases and have at least as great a capacity to account for the main fracture phenomena. To confirm this claim, the paper will focus on the ability of the cohesive force models to correct the three main flaws of Griffith's law of brittle fracture concerning the nucleation of cracks, the size effects or fatigue.

1. Introduction.

Griffith's brittle fracture theory developed from the seminal article Griffith (1921) remains until today the most widely used theory although it contains major flaws such as (i) its inability to account for initiation of a crack in a healthy elastic body, (ii) its prediction of unrealistic scale effects, (iii) its inability to take into account fatigue effects observed under cyclic loading. These defects essentially come from the too simple form adopted for the surface energy by assuming its proportionality to the area of the surface of discontinuity (the crack) whatever the amplitude of the jump of displacements on this crack.

To correct some of these defects, in particular the first concerning crack nucleation, damage mechanics has been developed. Since local damage models with stress softening contain the concept of maximum stress the material can sustain, unlike Griffith's theory which allows infinite stresses (which is a consequence of the choice of the surface energy), they had a chance to achieve it. However it was necessary to avoid an excessive damage localisation by introducing terms of gradient of damage in the energy. It turns out that such gradient damage models (commonly called phase field models in the literature) developed within the framework of the variational approach to fracture Bourdin et al. (2008) can really solve this problem and are also able to handle the tricky problem of arbitrary crack paths in a simple way. But for their part, these models are only based on purely phenomenological considerations and cannot be constructed from precise physical bases. Moreover, they leave the third flaw (concerning fatigue effects) largely unsolved.

There exists another way of correcting the defects of Griffith's theory: it consists in reintroducing the forces of cohesion between the lips of the cracks which are neglected in this theory. The consequence is that the surface energy density is no longer a constant, but depends on the jump of the displacement. This was essentially the idea of Dugdale Dugdale (1960) and Barenblatt Barenblatt (1962), even though they only made partial use of all the capabilities of this approach. Indeed, such a cohesive law contains both a critical stress and a characteristic length which could remedy the first two drawbacks. To solve the last one, relating to fatigue, it remains to introduce a condition of irreversibility inside the cohesive law, which probably constitutes the most delicate and debatable part of the construction of the models of cohesive forces. The goal of this paper is to show that, with all these ingredients, the cohesive force models are really able to fix the three drawbacks in a very convincing way. Therefore, we will focus on these objectives by considering examples or methods that are as simple as possible but also as generic as possible. We do not try to make a review, even a short one, of all the literature which was devoted to the models of cohesive forces.

Specifically, the paper is organised as follows. In Section 2 the three flaws of Griffith's theory are recalled and illustrated on a basic example, and the cohesive force models are introduced (without a condition of irreversibility). Section 3 is devoted to obtaining, by a stability argument, a local criterion formulated in term of the stresses for the nucleation of a cohesive crack in a sound body. In a three-dimensional isotropic framework, this leads to specific material strength properties which are discussed. In Section 4, an elementary but generic example shows how the cohesive force models correct the erroneous scale effects predicted by Griffith's law. Then the fundamental problem of the initiation of a "true" (*i.e.,* non-cohesive) crack at the tip of a notch is solved by a two scale approach. In the case of Dugdale's model, this problem is solved in closed form and an explicit formula gives the loading at which a "true" crack appears as function of the angle of the notch. Section 5 is devoted to the study of fatigue effects. First, an irreversibility condition is introduced and the induced changes in Dugdale's model are set. Then an explicit fatigue law of Paris-type is deduced from this Dugdale's model with irreversibility by using a two-scale approach. The paper finishes with a short conclusion and two appendices where the main steps for solving, via the theory of complex potentials, some specific elastic problems appearing throughout the paper are recalled.

From the technical standpoint, we essentially use classical methods of the Calculus of Variations like directional derivatives of functionals or integration by parts, we refer to the methods of complex analysis to solve some elementary two-dimensional elastic

jjmarigo@yahoo.fr (Jean-Jacques Marigo)
ORCID(s): 0000-0001-7949-5031 (Jean-Jacques Marigo)

problems, we use in an intuitive way two-scale approaches and we assume that the reader is familiar with the basic concepts of Fracture Mechanics like singularities, stress intensity factors or energetic concepts which can be found in any introductory textbook.

Throughout the paper, intrinsic vectorial notation are generally used: vectors and tensors are represented by boldface letters, their components by italic letters. The point $\cdot$ stands for the inner product of vectors or tensors: for instance, $\mathbf{v}\cdot\mathbf{v} = \sum_i v_i v_i$, $\boldsymbol{\sigma}\cdot\boldsymbol{\varepsilon} = \sum_{i,j} \sigma_{ij}\varepsilon_{ij}$. The norm of vectors, tensors or fields is represented by $\|\ \|$. Since all the analysis is made in the small displacement setting, $\boldsymbol{\varepsilon}(\mathbf{u})$ denotes the symmetrised gradient of $\mathbf{u}$ and represents the strain field associated with the displacement field $\mathbf{u}$, and $\boldsymbol{\sigma}$ is the stress tensor. When $\mathbf{u}$ is allowed to be discontinuous across a surface Γ whose normal is $\mathbf{n}$, the jump $[\![\mathbf{u}]\!](\mathbf{x})$ of $\mathbf{u}$ at $\mathbf{x}\in\Gamma$ is defined by

$$[\![\mathbf{u}]\!](\mathbf{x}) = \mathbf{u}^+(\mathbf{x}) - \mathbf{u}^-(\mathbf{x}), \qquad \mathbf{u}^\pm(\mathbf{x}) = \lim_{\{\mathbf{y}\to\mathbf{0}\,:\,\mathbf{y}\cdot\mathbf{n}(\mathbf{x})>0\}} \mathbf{u}(\mathbf{x}\pm\mathbf{y}).$$

2. The flaws of Griffith's theory and the introduction of cohesive forces

The hypothesis of Griffith on the surface energy is partially justified by physical considerations at an atomic scale. Indeed, if one considers a lattice of atoms whose interactions are governed by an interatomic potential of Lennard-Jones type, then after *complete separation* of two planes of atoms the lattice has an energy which is increased of an amount approximately proportional to the surface of separation, see figure 1. After separation, there is no longer any interaction between the two planes.

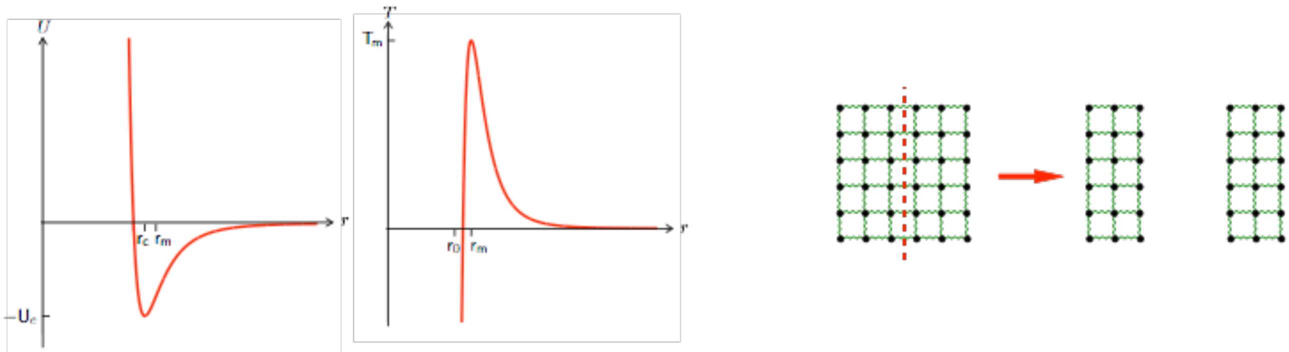

Figure 1: Lennard-Jones interaction potential and separation of two planes of atoms in a lattice

But this is not true as long as the separation is not complete. During this stage, the energy is gradually increased and forces of interaction exist. Accordingly, considering the lips of a crack from a macroscopic point of view, the cohesive forces the origin of which are the atomic forces of interaction can be neglected almost ewerywhere, except near the tip of the crack where the two lips are necessary close one to the other. In essence, it was the idea of Barenblatt to introduce these cohesive forces and hence to change the form of the surface energy. We will see that, even if the interactions between the lips exist only at short distances around the crack tip, they are sufficient to completely change many properties and to explain some phenomena that Griffith's theory misses. However, if the concept of cohesive forces originates from atomic considerations in a qualitative point of view, it is not possible to use directly the quantitative values given by the interatomic potentials because we would not obtain the good orders of magnitude. Therefore we are obliged to consider phenomenological cohesive laws and to identify them from specific experiments.

Specifically, we will consider in this paper, cohesive laws like those shown in figure 2: in a scalar setting, the surface energy density Φ is an increasing concave function of the displacement jump $[\![u]\!]$, which grows continuously from 0 to the constant $\mathsf{G_c}$ corresponding to the value of Griffith's model. At the same time, the cohesive forces which are given by the derivative of Φ, $\sigma = \Phi'([\![u]\!])$, are a decreasing function of the displacement jump. They decrease from $\sigma_c > 0$, the slope at 0 of the surface energy density, to 0. They vanish at a finite value of $[\![u]\!]$ or at infinity according to the model. In any case, such a cohesive model contains now not only the Griffith surface energy density $\mathsf{G_c}$ but also a characteristic stress σ_c and hence, automatically, a characteristic length δ_c given by the ratio $\mathsf{G_c}/\sigma_c$.

The simplest cohesive model which satisfies all the requirements is the model first proposed by Dugdale Dugdale (1960). The surface energy density grows linearly until it reaches the Griffith value $\mathsf{G_c}$. Hence the cohesive forces are piecewise constant and equal to σ_c until the jump of the displacement reaches the critical value δ_c, then cancel:

$$\Phi([\![u]\!]) = \begin{cases} \mathsf{G_c}\dfrac{[\![u]\!]}{\delta_c} & \text{if} \quad 0 \le [\![u]\!] \le \delta_c \\ \mathsf{G_c} & \text{if} \quad [\![u]\!] \ge \delta_c \end{cases}, \qquad \sigma := \Phi'([\![u]\!]) = \begin{cases} \sigma_c & \text{if} \quad 0 < [\![u]\!] < \delta_c \\ 0 & \text{if} \quad [\![u]\!] > \delta_c \end{cases}, \qquad \delta_c = \frac{\mathsf{G_c}}{\sigma_c}. \tag{1}$$

In the sequel, all the two-dimensional problems will be solved in a closed form by using this particular model. This will save us from having to resort to numerical computations and will allow us to discuss the influence of the parameters from explicit formulas.

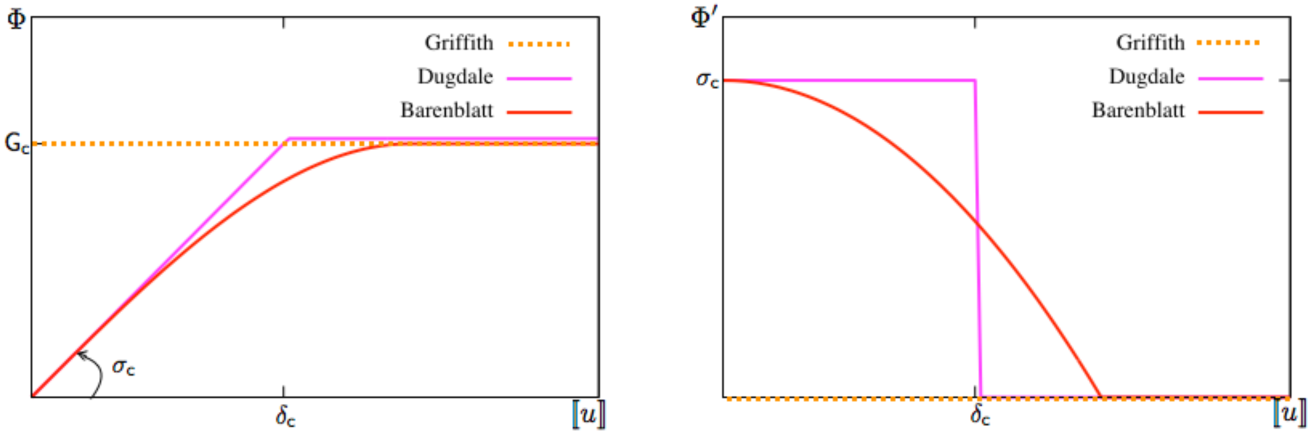

Figure 2: Densities of surface energy (left) and cohesive forces (right) in the models of Griffith, Dugdale and Barenblatt

Let us finish this section by showing the three main flaws of Griffith's law through an elementary but generic example. Let us consider, in plane strain, the infinite strip represented in figure 3, the width of which is $2L$, which contains a transverse centered crack of length 2ℓ and which is submitted to a uniform tensile stress at infinity in the direction orthogonal to the crack. The material is linear elastic and isotropic, with Young modulus E and Poisson ratio ν. We assume that the crack evolution is governed by Griffith's law. The

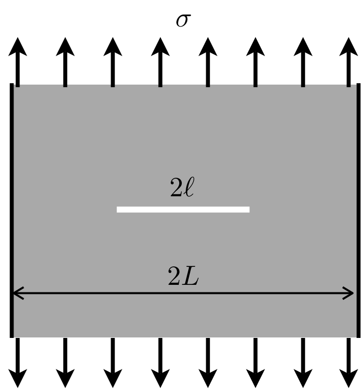

Figure 3: The cracked strip with its loading

crack is in mode I and the stress intensity factor K_I (the same at the two tips of the crack) can be obtained in a closed form and is given by

$$\mathsf{K}_\mathrm{I} = \sigma\sqrt{\frac{\pi\ell}{\cos\frac{\pi\ell}{2L}}}.$$

By using Irwin's formula, we deduce the potential energy release rate G that we have to compare to G_c:

$$G = \frac{1-\nu^2}{\mathsf{E}}{\mathsf{K}_\mathrm{I}}^2 = \frac{(1-\nu^2)\pi\ell}{\cos\dfrac{\pi\ell}{2L}}\frac{\sigma^2}{\mathsf{E}}.$$

Therefore the maximal stress σ_M that this strip can sustain is given by

$$\sigma_M = \sqrt{\frac{\mathsf{E}G_c}{1-\nu^2}\frac{\cos\frac{\pi\ell}{2L}}{\pi\ell}}. \tag{2}$$

Let us show the three defects of Griffith's law from this formula.

(i) *Bad size effects at small scale.* For a given ratio ℓ/L between the length of the crack and the width of the strip, σ_M goes to 0 like $1/\sqrt{L}$ when L goes to infinity. This size effect at large scale conforms to what is observed for a large class of brittle materials, see Bazant and Planas (1998). On the other hand, (2) also predicts that σ_M goes to infinity like $1/\sqrt{L}$ when L goes to 0, which is clearly unrealistic. Accordingly, Griffith's law predicts erroneous size effects at small scale.

(ii) *Non nucleation of cracks.* Now fix L and let ℓ tend to 0. Then G tends to 0 like ℓ and σ_M tends to infinity like $1/\sqrt{\ell}$. Thus it is not possible to nucleate a crack in a sound strip because the potential energy release rate is null regardless of the amplitude of the loading.

(iii) *No fatigue.* Let us assume that the strip is submitted to a cyclic loading, the stress at infinity σ oscillating between 0 and σ_m. Let us analyse what is predicted by Griffith's law according to whether σ_m is greater or smaller than σ_M. If $\sigma_m \geq \sigma_M$, then the strip will break during or at the end of the first loading phase. But if $\sigma_m < \sigma_M$, then the crack will never propagate regardless of the number of cycles. It is not possible to account for fatigue effects.

All these bad properties are generic in Griffith's theory and can be seen in any situation, they are not specific to this particular case. We will see that, by changing the surface energy and replacing Griffith's hypothesis by a Barenblatt surface energy, all these flaws are corrected.

3. The stress criterion of nucleation of a cohesive crack in Barenblatt's approach

Cohesive force models were first introduced in Dugdale (1960); Barenblatt (1962) to correct some flaws in Griffith's theory for a pre-existing crack. For example, in the case of the strip in figure 3, they are used to eliminate the singularity at the crack tip and to change the shape of the deformed configuration near the crack tip. Then, they were essentially used at given interfaces or for a given crack path. Here we will take a radically different view and consider that cohesive cracks (and ultimately non-cohesive cracks too) are free to arise and propagate anywhere in the body. The criterion which decides whether a crack must nucleate or not, propagate or not, will be a criterion of stability. This is essentially the fundamental idea developed in the variational approach to fracture Bourdin et al. (2008). We will apply this idea here to obtain a criterion of nucleation of a cohesive crack in a three-dimensional body. To simplify the presentation, we just consider the main steps of the analysis of stability and the arguments will be essentially formal. The reader interested by a more rigorous approach and by all the details of the procedure must consult Charlotte et al. (2006); Bourdin et al. (2008).

3.1. The stability condition and surface energy assumptions

Let Ω be the reference configuration of a homogeneous body which is made of an isotropic linearly elastic material characterised by its stiffness tensor A and which is submitted to a loading characterised by body forces $\mathbf{f}$, surface forces $\mathbf{F}$ applied on the part $\partial_F\Omega$ of the boundary of the domain and prescribed displacements $\mathbf{U}$ on the complementary part $\partial_D\Omega$ of the boundary. (The analysis of stability which follows could be extended practically without any change to nonlinear elastic materials.) Cohesive cracks governed by a law of Barenblatt's type can appear and propagate inside the body. Starting from the assumption that the body does not contain any crack and hence that the response is purely elastic, the goal of this section is to study the stability of the elastic response only. One advantage to limit the stability analysis to the nucleation of a cohesive crack in a sound body is that it does not require the introduction at this stage of an irreversibility condition.

Since the stability condition is based on energetic considerations, one must first define the energy of the body when its displacement field is $\mathbf{v}$. Since the displacements are allowed to be discontinuous across (arbitrary) surfaces, we denote by $S_\mathbf{v}$ the oriented surface of discontinuity of $\mathbf{v}$ (also called the jump set of $\mathbf{v}$), $\mathbf{n}$ the normal to that surface and $[\![\mathbf{v}]\!]$ the jump of $\mathbf{v}$ on it. Even if $\mathbf{v}$ can be discontinuous anywhere, its jump must satisfy the non-interpenetration condition which in our small displacement context simply requires that the normal jump be non negative:

$$[\![\mathbf{v}]\!]\cdot\mathbf{n} \geq 0 \quad on \quad S_\mathbf{v}. \tag{3}$$

The energy of the body consists of three contributions: the elastic energy, the surface energy and the potential energy due to the applied forces. Formally,

$$\mathcal{E}(\mathbf{v}) = \int_{\Omega\setminus S_\mathbf{v}} \frac{1}{2}\mathsf{A}\varepsilon(\mathbf{v})\cdot\varepsilon(\mathbf{v})dx + \int_{S_\mathbf{v}} \Phi(\mathbf{n},[\![\mathbf{v}]\!])dS - \mathsf{W_e}(\mathbf{v}). \tag{4}$$

In (4), $\mathsf{W}_e(\mathbf{v})$ is simply the work of the applied forces through $\mathbf{v}$,

$$\mathsf{W_e}(\mathbf{v}) = \int_\Omega \mathbf{f}\cdot\mathbf{v}dx + \int_{\partial_F\Omega} \mathbf{F}\cdot\mathbf{v}dS,$$

while $\Phi(\mathbf{n},[\![\mathbf{v}]\!])$ denotes the surface energy density which in a fully three-dimensional context depends non only on the jump of the displacement but also on the orientation of the surface of discontinuity (the non-interpenetration condition (3) suffices to force that dependence). For the elastic response $\mathbf{u}$, which by definition is not discontinuous, the energy contains two terms only, since the surface energy cancels:

$$\mathcal{E}(\mathbf{u}) = \int_\Omega \frac{1}{2}\mathsf{A}\varepsilon(\mathbf{u})\cdot\varepsilon(\mathbf{u})dx - \mathsf{W}_e(\mathbf{u}).$$

The stability criterion consists to compare the energy of the body in its tested state to the energy of the body in a slightly perturbed state *accessible* from the tested one. The physical justification of this definition is that the body cannot be in a certain state, if there is a state close to it and accessible from it with lower energy. Accessibility constraints come from kinematic boundary conditions, kinematic constraints or irreversibility conditions. This general principle can be applied to any physical system where there exists an energy associated to a state. In mechanics, this is the case for conservative systems but also for a class of dissipative systems. For instance, it can be used for rate independent constitutive laws like plasticity, brittle damage or brittle fracture provided that they correspond to standard laws in the sense of Generalized Standard Materials, see Mielke (2005). In particular, in brittle fracture with Griffith's surface energy, the stability consists in testing the stability of a crack state of a body by adding a small crack surface and by comparing the total energy of the body in this new crack state with its energy in the previous one. At first order, this comparison leads in particular to the usual Griffith criterion of propagation $G \le \mathsf{G_c}$, but it is possible to obtain additional criteria by testing for instance the branching of a crack, see Chambolle et al. (2009). Here, in the context of cohesive force models, the procedure can still be applied, but due to the change of the form of the surface energy we must reconsider all its steps.

The tested state is the elastic response at equilibrium $\mathbf{u}$. The displacement fields which can be used to test the stability of $\mathbf{u}$ are the displacement fields $\mathbf{v}$ close to it (in a sense to be specified) which verify the kinematic conditions on $\partial_D\Omega$ and which can be discontinuous *anywhere*, on *any surface* and with *an arbitrary (but small) jump* provided that the jump satisfies *the non-interpenetration condition*. Accordingly, the stability condition reads as

$$\mathcal{E}(\mathbf{u}) \le \mathcal{E}(\mathbf{v}), \forall \mathbf{v} \text{ close to } \mathbf{u} \text{ such that } \mathbf{v} = \mathbf{U} \text{ on } \partial_D\Omega,\ [\![\mathbf{v}]\!]\cdot\mathbf{n} \ge 0 \text{ on } S_\mathbf{v}. \tag{5}$$

The stability condition will be used with a particular family of displacement tests once the properties of the surface energy density have been specified. We assume that the material is isotropic and hence the surface energy density Φ must satisfy $\Phi(\mathbf{Qn},\mathbf{Q}\boldsymbol{\delta}) = \Phi(\mathbf{n},\boldsymbol{\delta})$ for all orthogonal matrix $\mathbf{Q}$, all unit vector $\mathbf{n}$ and all vector $\boldsymbol{\delta}$. This is possible if and only if the surface energy density only depends on the invariants of $(\mathbf{n},\boldsymbol{\delta})$. Since $\mathbf{n}$ is of norm 1, these invariants are $\boldsymbol{\delta}\cdot\mathbf{n}$ and $\|\boldsymbol{\delta}\|$, or equivalently, $\boldsymbol{\delta}\cdot\mathbf{n}$ and $\|\boldsymbol{\delta} - \boldsymbol{\delta}\cdot\mathbf{n}\,\mathbf{n}\|$. Moreover, the non-interpenetration condition requires that $\boldsymbol{\delta}\cdot\mathbf{n} \ge 0$. Consequently, there exists a function ϕ defined for positive values of its two arguments such that the surface energy density reads as

$$\Phi(\mathbf{n},\boldsymbol{\delta}) = \phi(\boldsymbol{\delta}\cdot\mathbf{n}, \|\boldsymbol{\delta} - \boldsymbol{\delta}\cdot\mathbf{n}\,\mathbf{n}\|) \text{ with } \boldsymbol{\delta}\cdot\mathbf{n} \ge 0. \tag{6}$$

Moreover the function ϕ is non negative and vanishes only at $(0,0)$. The use of the stability condition requires to make some hypotheses concerning the differentiability of ϕ at $(0,0)$. Here we assume that ϕ admits directional derivatives at the origin, *i.e.,* there exists a positive, one-homogeneous function φ such that for all non negative pairs $(\alpha,\beta) \ne (0,0)$,

$$0 < \varphi(\alpha,\beta) = \lim_{h\downarrow 0}\frac{1}{h}\phi(h\alpha,h\beta), \qquad \varphi(\lambda\alpha,\lambda\beta) = \lambda\varphi(\alpha,\beta), \forall\lambda > 0. \tag{7}$$

In particular, we denote by σ_c and τ_c the partial derivatives:

$$\sigma_c = \varphi(1,0) > 0, \quad \tau_c = \varphi(0,1) > 0. \tag{8}$$

We will distinguish the particular case when ϕ is differentiable at $(0,0)$. In such a case φ is linear: $\varphi(\alpha,\beta) = \sigma_c\alpha + \tau_c\beta$.

3.2. The stress yield criterion

3.2.1. Deduction of the stress yield criterion from the stability condition

Let us define the family of displacement fields $\mathbf{v}_h$, where h is a small positive parameter, used to test the stability of $\mathbf{u}$. Let $\mathbf{x}_0$ be an arbitrary point chosen in Ω, $\mathbf{n}$ an arbitrary unit vector, $\boldsymbol{\delta}$ an arbitrary vector such that $\boldsymbol{\delta}\cdot\mathbf{n} \ge 0$, and let η be a smooth positive function such that $\eta(0) = 1$ and whose support is included in $(-d,+d)$ with d small enough in order that the ball of center $\mathbf{x}_0$ and radius d be included in Ω. Then $\mathbf{v}_h$ is defined by

$$\mathbf{v}_h(\mathbf{x}) = \mathbf{u} + h\mathbf{w}, \qquad \mathbf{w}(\mathbf{x}) = H((\mathbf{x}-\mathbf{x}_0)\cdot\mathbf{n})\eta(\|\mathbf{x}-\mathbf{x}_0\|)\boldsymbol{\delta}, \tag{9}$$

where H denotes the Heaviside function, *i.e.,* $H(x) = 0$ if $x \le 0$, $H(x) = 1$ otherwise. Hence, $\mathbf{v}_h$ differs from $\mathbf{u}$ only in the ball of center $\mathbf{x}_0$ and radius d. Therefore, $\mathbf{v}_h$ satisfies the kinematic boundary conditions. Moreover, the jump set of $\mathbf{v}_h$ is that of $\mathbf{w}$ and is the disk centered on $\mathbf{x}_0$ with radius d and normal $\mathbf{n}$. The jump vector of $\mathbf{v}_h$ on $S_\mathbf{w}$ is given by $[\![\mathbf{v}_h]\!] = h[\![\mathbf{w}]\!]$, with $[\![\mathbf{w}]\!](\mathbf{x}) = \eta(\|\mathbf{x}-\mathbf{x}_0\|)\boldsymbol{\delta}$, and hence is parallel to $\boldsymbol{\delta}$ with a norm of the order of h. Therefore, $\mathbf{v}_h$ satisfies the non-interpenetration condition and we will consider that $\mathbf{v}_h$ is close to $\mathbf{u}$ because h is small. Since $\mathbf{v}_h$ is an accessible small perturbation, one can use it as a displacement field testing the stability of $\mathbf{u}$. Starting from (5) with $\mathbf{v} = \mathbf{v}_h$, dividing by h and passing to the limit leads to the following inequality

$$\int_{\Omega\setminus S_{\mathbf{w}}} \boldsymbol{\sigma} \cdot \boldsymbol{\varepsilon}(\mathbf{w}) dx + \int_{S_{\mathbf{w}}} \varphi(\llbracket\mathbf{w}\rrbracket\cdot\mathbf{n}, \|\llbracket\mathbf{w}\rrbracket - \llbracket\mathbf{w}\rrbracket\cdot\mathbf{n}\,\mathbf{n}\|) dS - \int_{\Omega} \mathbf{f} \cdot \mathbf{w} dx - \int_{\partial_F\Omega} \mathbf{F} \cdot \mathbf{w} dS \geq 0. \tag{10}$$

To obtain (10), one must calculate the directional derivative of the energy $\mathcal{E}$ which involves itself the directional derivatives of ϕ, which explains the presence of φ. After integrating by parts the first integral in (10) and taking into account the equilibrium equations satisfied by the stress tensor field $\boldsymbol{\sigma}$,

$$\mathbf{div}\sigma + \mathbf{f} = \mathbf{0} \text{ in } \Omega, \quad \boldsymbol{\sigma}\mathbf{n} = \mathbf{F} \text{ on } \partial_F\Omega,$$

all terms disappear except for the integral over the jump set of $\mathbf{w}$. Specifically, one gets

$$\int_{S_{\mathbf{w}}} \boldsymbol{\sigma}\mathbf{n} \cdot \llbracket\mathbf{w}\rrbracket dS \leq \int_{S_{\mathbf{w}}} \varphi(\llbracket\mathbf{w}\rrbracket\cdot\mathbf{n}, \|\llbracket\mathbf{w}\rrbracket - \llbracket\mathbf{w}\rrbracket\cdot\mathbf{n}\,\mathbf{n}\|) dS.$$

Moreover, using the one-homogeneity of φ and inserting the expression of $\llbracket\mathbf{w}\rrbracket$ into the above inequality leads to

$$\int_{S_{\mathbf{w}}} \Big(\boldsymbol{\sigma}(\mathbf{x})\mathbf{n} \cdot \boldsymbol{\delta} - \varphi(\boldsymbol{\delta} \cdot \mathbf{n}, \|\boldsymbol{\delta} - \boldsymbol{\delta}\cdot\mathbf{n}\,\mathbf{n}\|)\Big)\eta(\|\mathbf{x} - \mathbf{x}_0\|) dS \leq 0. \tag{11}$$

Since η is an arbitrary positive smooth function, by standard arguments of the Calculus of Variations, one can drop the integral in (11) to obtain the following local inequality which must hold almost everywhere in Ω because $\mathbf{x}_0$ is arbirary:

$$\boldsymbol{\sigma}\mathbf{n} \cdot \boldsymbol{\delta} \leq \varphi(\boldsymbol{\delta} \cdot \mathbf{n}, \|\boldsymbol{\delta} - \boldsymbol{\delta}\cdot\mathbf{n}\,\mathbf{n}\|).$$

By homogeneity, one can divide by the norm of $\boldsymbol{\delta}$, and since $\mathbf{n}$ and $\boldsymbol{\delta}$ have been chosen arbitrarily one finally obtains the following local condition, called *the yield stress criterion*, that the stress tensor must satisfy:

$$\boxed{\boldsymbol{\sigma}\mathbf{n} \cdot \boldsymbol{\delta} \leq \varphi(\boldsymbol{\delta} \cdot \mathbf{n}, \|\boldsymbol{\delta} - \boldsymbol{\delta} \cdot \mathbf{n}\,\mathbf{n}\|), \quad \forall (\mathbf{n}, \boldsymbol{\delta}) : \|n\| = \|\boldsymbol{\delta}\| = 1, \boldsymbol{\delta} \cdot \mathbf{n} \geq 0.} \tag{12}$$

Let us comment on this result:

- It is because the cracks are *free* surface of discontinuities that the inequality (12) must hold at any point, in any direction and for any jump compatible with the non-interpenetration condition. The use of the same procedure in the case of a prescribed interface removes the "for any point and any direction".
- The inequality is *local* and hence it does not depend on the particular problem considered. It does not depend on the choice of the domain, the type of loading , or the whole elastic response. If one changes the body and the loading, the stability condition will always lead to the same inequality. Therefore, the yield stress criterion must be considered as a property of the material: isotropic material which can host cracks with such a cohesive law cannot sustain stresses which violate the inequality (12). In other words, *the stability condition allows us to deduce the strength of the material from the surface energy density*.
- We could consider the case when the body is already cracked. By testing only the zone which is still sound, we would recover the same inequality in that zone.
- In one dimension the inequality (12) reduces to
$$\sigma \leq \sigma_c = \Phi'(0).$$
Therefore the slope at 0 of the surface energy density is the maximal stress that the material can sustain. This property was first established by Del Piero (1999); Charlotte et al. (2000) with practically the same procedure.

3.2.2. Properties of the yield surface

We briefly recall in this subsection the most important properties of the yield stress criterion (12), the reader interested in the details of the proofs can refer to Charlotte et al. (2006). The eigenstresses of the stress tensor $\boldsymbol{\sigma}$ are denoted $\sigma_i, 1 \leq i \leq 3$, and ordered as follows:

$$\sigma_1 \leq \sigma_2 \leq \sigma_3.$$

(i) Case when the surface energy density is differentiable at the origin. In such a case φ is linear and the yield stress criterion (12) becomes

$$\boldsymbol{\sigma}\mathbf{n} \cdot \boldsymbol{\delta} \leq \sigma_c \boldsymbol{\delta}\cdot\mathbf{n} + \tau_c \|\boldsymbol{\delta} - \boldsymbol{\delta}\cdot\mathbf{n}\,\mathbf{n}\| \tag{13}$$

where the inequality must hold for all unit vectors $\mathbf{n}$ and $\boldsymbol{\delta}$ such that $\boldsymbol{\delta}\cdot\mathbf{n} \geq 0$. Let $\mathbf{n}$ be a given unit vector and let us decompose $\boldsymbol{\delta}$ in its normal and tangential part, $\boldsymbol{\delta} = \cos\theta\,\mathbf{n} + \sin\theta\,\mathbf{t}$ where $\theta \in [-\pi/2, \pi/2]$ and $\mathbf{t}$ is a unit vector orthogonal to $\mathbf{n}$. Inserting into (13) gives

$$(\boldsymbol{\sigma}\mathbf{n}\cdot\mathbf{n} - \sigma_c)\cos\theta + \boldsymbol{\sigma}\mathbf{n}\cdot\mathbf{t}\sin\theta - \tau_c\,|\sin\theta| \leq 0, \quad \forall\theta \in [-\pi/2, \pi/2], \quad \forall(\mathbf{n},\mathbf{t}) : \|\mathbf{n}\| = \|\mathbf{t}\| = 1, \mathbf{n}\cdot\mathbf{t} = 0. \tag{14}$$

Then, it is easy to show that (14) is equivalent to $\max_{\mathbf{n}} \boldsymbol{\sigma}\mathbf{n}\cdot\mathbf{n} \leq \sigma_c$ and $\max_{(\mathbf{n},\mathbf{t}):\mathbf{n}\cdot\mathbf{t}=0} \boldsymbol{\sigma}\mathbf{n}\cdot\mathbf{t} \leq \tau_c$, and finally to

$$\sigma_3 \leq \sigma_c \quad \text{and} \quad \sigma_3 - \sigma_1 \leq 2\tau_c. \tag{15}$$

We have thus obtained the following property:

Property 1. *When the surface energy density ϕ is differentiable at the origin, the yield stress criterion given by the first order stability conditions consists of a maximal tension criterion and a maximal shear criterion, the maximal tension σ_c and the maximal shear τ_c that the material can sustain being given by the partial derivatives of ϕ at the origin.*

(ii) Case when the surface energy density is not differentiable at the origin. It is the general case and φ is only one-homogeneous. Then we obtain the following property, the proof of which can be found in Charlotte et al. (2006):

Property 2 (Intrinsic curve). *For a given stress tensor $\boldsymbol{\sigma}$ and a given unit vector $\mathbf{n}$, let us decompose the stress vector $\boldsymbol{\sigma}\mathbf{n}$ into its normal and tangential parts:*

$$\boldsymbol{\sigma}\mathbf{n} = \Sigma\mathbf{n} + T\mathbf{t} \tag{16}$$

where $\mathbf{t}$ is a unit vector orthogonal to $\mathbf{n}$. Then, $\boldsymbol{\sigma}\mathbf{n}$ satisfies the following inequality

$$\boldsymbol{\sigma}\mathbf{n} \cdot \boldsymbol{\delta} \leq \varphi(\boldsymbol{\delta}\cdot\mathbf{n}, \|\boldsymbol{\delta} - \boldsymbol{\delta}\cdot\mathbf{n}\,\mathbf{n}\|), \quad \forall\boldsymbol{\delta} : \|\boldsymbol{\delta}\| = 1, \boldsymbol{\delta}\cdot\mathbf{n} \geq 0$$

if and only if *the stress vector (Σ, T) lies in the following convex set of the Mohr diagram:*

$$|T| \leq \varphi_\star(\Sigma) = \inf_{\lambda\geq 0}\{\varphi(\lambda, 1) - \lambda\Sigma\}. \tag{17}$$

Moreover the function $\varphi_\star$ giving the so-called intrinsic curve *$|T| = \varphi_\star(\Sigma)$ enjoys the following properties:*

1. *The function $\varphi_\star$ is defined for $\Sigma \in (-\infty, \sigma_c)$, concave, continuous, decreasing, and such that $\lim_{\Sigma\to-\infty} \varphi_\star(\Sigma) = \tau_c = \varphi(0, 1)$. Further, $\varphi_\star$ is non negative for $\Sigma \in (-\infty, \sigma_c^\star]$ and vanishes at $\sigma_c^\star \leq \sigma_c = \varphi(1, 0)$.*
2. *The domain of the admissible (Σ, T) delimited by the intrinsic curve is convex, symmetric with respect to the axis $T = 0$, unbounded in the direction of negative normal stress and bounded by $\sigma_c^\star$ in the direction of positive normal stress, see Figure 4.*

In the previous property the normal $\mathbf{n}$ is fix. But the yield stress criterion must be satisfied for any $\mathbf{n}$, so we have now to consider all the $\mathbf{n}$'s. This leads to the introduction of Mohr's circles. Indeed, for a given $\boldsymbol{\sigma}$, when $\mathbf{n}$ describes the unit sphere, the stress vector $\boldsymbol{\sigma}\mathbf{n}$ describes the domain delimited by the three Mohr circles in the Mohr diagram (these are the circles centered on the axis $T = 0$ and passing through the three points $(\sigma_i, 0)$, $1 \leq i \leq 3$). Consequently, in order that $\boldsymbol{\sigma}$ satisfies the yield stress criterion for all $\mathbf{n}$, the greatest Mohr circle (the one passing through $(\sigma_1, 0)$ and $(\sigma_3, 0)$) must be inside the domain delimited by the intrinsic curve. Finally, the set of admissible stress tensors is the convex hull of all greatest circles that lie inside that domain. This leads to the final property characterising the admissible stress tensors:

Property 3. *The set of stress tensors $\boldsymbol{\sigma}$ satisfying the yield stress criterion (12) is such that*

$$\frac{\sigma_3 - \sigma_1}{2} \leq \varphi^\star\left(\frac{\sigma_1 + \sigma_3}{2}\right) \quad \textit{with} \quad \varphi^\star(s) = \inf_{\theta\in[0,\pi/2]}\{\varphi(\cos\theta, \sin\theta) - s\cos\theta\}. \tag{18}$$

The above inequality gives the maximal allowable radius of the greatest Mohr circle as a function of the position of its center.

Let us comment on these results:

- The domain that defines the strength of the material is given by the slopes of the surface energy function ϕ at the origin. It is therefore essential that these slopes be positive. Indeed, if $\tau_c = 0$, then the material cannot sustain *any* shear stress; if $\sigma_c = 0$, then the material cannot support *any* tension. This requirement comes from the condition of stability and the fact that cracks are free to appear anywhere. Therefore, if one uses cohesive force models in which the slopes of the surface energy at the origin cancel, then the material will behave as a fluid without shear stress and only under positive pressure. In other words, this remark disqualifies all the so-called intrinsic cohesive models.

- The strength criterion is asymmetric in tension and compression simply because of the non-interpenetration condition.
- By construction the envelope of greatest Mohr circles does not depend on the intermediate eigenstress σ_2 but only on the extremal eigenstresses σ_1 and σ_3. This could be considered too restrictive as it excludes criteria like the Von Mises criterion. Let us remember, however, that this is a local criterion. Thus in a heterogeneous material with a fine microstructure, the effective (in the sense of observed macroscopically) criterion will depend on all the three macroscopic eigenstresses.
- It should be emphasised that we find the strength criteria based on the concepts of Mohr circles and intrinsic curves that engineers have proposed during the last century from empirical considerations. Here they are the byproduct of a stability condition, a hypothesis of isotropy of the material and a weak assumption on the smoothness of the surface energy density.
- In (phase field or) gradient damage models like the Ambrosio-Tortorelli model or one of its variants, the stress criterion which governs the onset of damage corresponds to ellipsoids in the set of stress tensors when the material is assumed to have a linear elastic behaviour at given damage state. To obtain more general yield surfaces one must introduce a nonlinear behaviour of the material, see Amor et al. (2009). Consequently, it is practically impossible to construct damage models leading to yield surfaces like those obtained with cohesive models.

3.2.3. Some examples of yield surface

(i) Case when φ is concave and continuous. Then the minimum of $\varphi(\cos\theta, \sin\theta) - s\cos\theta$ over $[0, \pi/2]$ is reached at the boundary, *i.e.,* either at $\theta = 0$ or at $\theta = \pi/2$. Hence $\varphi^\star(s) = \min\{\sigma_c - s, \tau_c\}$ and we recover the maximal tension and the maximal shear criteria as in the case where φ is linear.

(ii) A case when φ convex. Let φ be the convex function defined by

$$\varphi(\alpha, \beta) = 2\sqrt{\sigma_c^2\alpha^2 + \tau_c^2\beta^2} - \sigma_c\alpha - \tau_c\beta. \tag{19}$$

After some calculations, one gets

$$\varphi_\star(\Sigma) = \begin{cases} \tau_c & \text{if } \Sigma \le -\sigma_c \\ \tau_c\left(\sqrt{4 - \left(1 + \dfrac{\Sigma}{\sigma_c}\right)^2} - 1\right) & \text{if } -\sigma_c \le \Sigma \le \sigma_c \end{cases}. \tag{20}$$

Thus, $\varphi_\star$ is positive if and only if $\Sigma \le (\sqrt{3} - 1)\sigma_c \equiv \sigma_c^\star$ and $\sigma_c^\star$ is the maximal tension that the material can sustain. The intrinsic curve, represented on Figure 4, is made of a line segment and an arc of an ellipse.

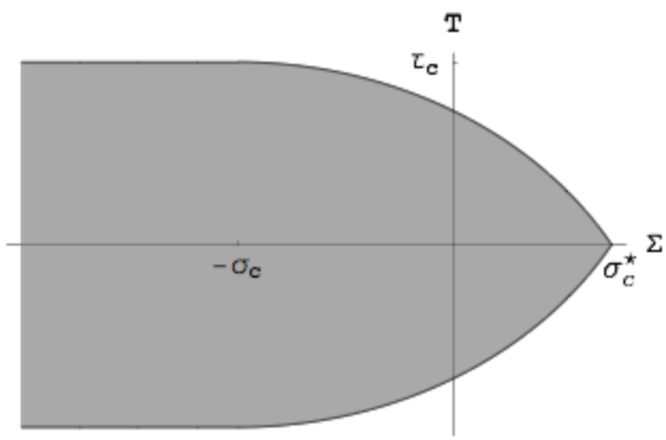

Figure 4: The set of the admissible stress vectors in the Mohr diagram in the case where φ is given by (19).

4. Initiation of non-cohesive cracks and size effects

4.1. Corrected size effects

Let us show on an elementary but illuminating example that the introduction of a critical stress and a characteristic length in a cohesive model allows us to fix the erroneous size effects predicted by Griffith's theory. Consider an infinite two-dimensional medium which contains a preexisting crack of length 2ℓ (the cut) along the axis $x_2 = 0$. The medium is made of an isotropic material with Young modulus E and Poisson ratio ν and is submitted to a uniform tension σ_∞ at infinity in the direction 2, see figure 5. All the calculations are made in the plane strain setting.

In Griffith's theory, the cut is in mode I and the stress intensity factor $\mathsf{K_I}$ at the two tips A and A' of the cut is given by the well known formula $\mathsf{K_I} = \sigma_\infty\sqrt{\pi\ell}$. Hence, using Irwin's formula, the potential energy release rate G is given by $G = \frac{1-\nu^2}{\mathsf{E}}\sigma_\infty^2\pi\ell$. From the Griffith criterion one deduces that the initial crack will propagate as soon as σ_∞ reaches the critical value σ_G given by

$$\sigma_G = \sqrt{\frac{\mathsf{G_c E}}{(1-\nu^2)\pi\ell}}.$$

Moreover, the propagation of the crack is then brutal, the medium cannot sustain a loading greater than σ_G and hence will break at σ_G. We see that the failure stress varies like $1\sqrt{\ell}$, which conforms to the size effect previously announced.

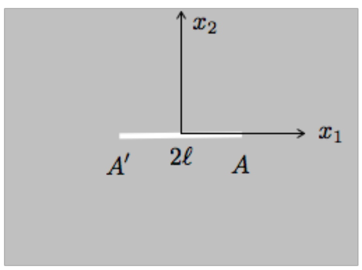

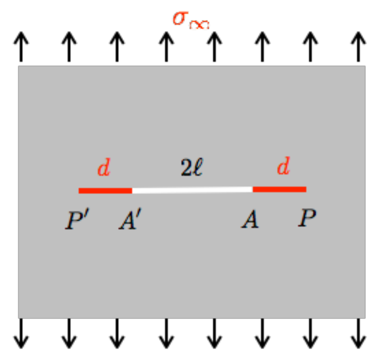

Figure 5: The initial cut (left) and the cut with a cohesive crack at its tips after loading (right)

Let us now assume that the evolution of the crack is governed by Dugdale's model. By symmetry, we only consider a propagation of the crack along the axis $x_2 = 0$ and symmetric with respect to the axis $x_1 = 0$. Hence, only the component u_2 of the displacement will be discontinuous and we will use (1) with $u = u_2$ and $\sigma = \sigma_{22}$. Let us describe the scenario of propagation of the crack:

1. As soon as a loading $\sigma_\infty > 0$ is prescribed, a cohesive crack will appear at the tips A and A' of the cut. Indeed, the elastic response is singular at both ends with a stress intensity factor $\mathsf{K_I} = \sigma_\infty\sqrt{\pi\ell}$. But by virtue of the stability condition, we have shown is the previous section that the material cannot sustain a stress σ_{22} greater than σ_c. Hence a cohesive crack must appear the length d of which (the same at the two ends) has to be determined, see figure 5.

2. For a small enough value of σ_∞, the cohesive forces will be equal to σ_c (*i.e.,* $\sigma_{22} = \sigma_c$) along the cohesive part of the crack, that is for $\ell < |x_1| < \ell + d$ by virtue of Dugdale's law. Accordingly, the displacement and the stress fields will be obtained by solving an elastic problem on the infinite domain without the crack line ($|x_1| \le \ell + d, x_2 = 0$), with σ_{22} given, piecewise constant on this line (and $\sigma_{12} = 0$) and $\boldsymbol{\sigma}$ given at infinity. *A priori*, such a response is singular at the tips P and P' with some value $\mathsf{K_I}(P) = \mathsf{K_I}(P')$ of the stress intensity factor. But, once more, since the material cannot sustain a normal stress greater than σ_c, the stress intensity factor must vanish. The equation $\mathsf{K_I}(P) = 0$ will give us the length d of the cohesive part of the crack as a function of the loading σ_∞. In other words, the length of the cohesive crack must be adjusted in order to eliminate the singularity at P and P'. It turns out that this elastic problem can be solved in closed form by techniques using complex analysis, as the one described in the appendices. The calculations are not reproduced here, and one eventually obtains that $\mathsf{K_I}(P)$ is given by

$$\mathsf{K_I}(P) = \sigma_\infty\sqrt{\pi(\ell+d)} - 2\sigma_c\sqrt{\frac{\ell+d}{\pi}}\arccos\frac{\ell}{\ell+d}.$$

   It is interesting to see the opposite influences of the loading and the cohesive forces in this formula. The first term in the right hand side is positive and due to the loading. Its contribution to the stress intensity factor is the same as in the case of a non-cohesive crack of length $2(\ell+d)$. The second term is negative and due to the cohesive forces which tend to close the crack. When d is small the first term is dominant (the second goes to 0 when d goes to 0); when d is large, it is the converse, the second term becomes dominant (provided that $\sigma_\infty < \sigma_c$). So, there exists only one value of d for which the two terms are balanced, it corresponds to the searched length of the cohesive crack. Therefore, d is given by

$$\ell + d = \frac{\ell}{\cos\left(\dfrac{\pi}{2}\dfrac{\sigma_\infty}{\sigma_c}\right)}. \tag{21}$$

The dependence of the cohesive crack length on the loading can be seen in figure 6, d is an increasing function of σ_∞, growing from 0 to infinity when σ_∞ grows from 0 to σ_c.

3. The previous calculations are valid as long as the opening of the crack at A and A' is less than the critical opening δ_c of Dugdale's law. Indeed, the cohesive forces are equal to σ_c only when $[\![u_2]\!] < \delta_c$. Since $[\![u_2]\!](x_1)$ is a decreasing function of $|x_1|$, decreasing from $[\![u_2]\!](\ell)$ to 0 when $|x_1|$ increases from ℓ to $\ell + d$, we simply have to compare the value of $[\![u_2]\!](\ell)$ to δ_c. Since the problem can be solved in closed form, one finally gets

$$[\![u_2]\!](\ell) = -\frac{8}{\pi}(1-\nu^2)\log\cos\left(\frac{\pi}{2}\frac{\sigma_\infty}{\sigma_c}\right)\frac{\sigma_c}{\mathsf{E}}\ell, \tag{22}$$

where we have taken into account that the length of the cohesive crack is given by (21). Therefore the previous calculations are valid as long as σ_∞ does not reach the critical value σ_D given by

$$\sigma_D = \frac{2}{\pi}\arccos\left(\exp\left(-\frac{\mathsf{d_c}}{\ell}\right)\right)\sigma_c \quad \text{with} \quad \mathsf{d_c} = \frac{\pi}{8(1-\nu^2)}\frac{\mathsf{EG_c}}{\sigma_c^2}. \tag{23}$$

4. Let us show that σ_D is the maximal loading that the medium can sustain. Indeed, let us consider a loading σ_∞ greater than σ_D. Then necessarily a non-cohesive crack should appear at the tips A and A' because the opening at these points becomes greater than δ_c. Let $2\ell' > 2\ell$ be the new length of the non-cohesive crack, and B and B' its tips. The opening at B and B' should be equal to δ_c, the length d' of the non-cohesive part of the crack would be given by (21) with d' and ℓ' instead of d and ℓ. We could use (22) with ℓ' instead of ℓ to obtain the opening at B. Accordingly, we should have

$$\sigma_\infty = \frac{2}{\pi}\arccos\left(\exp\left(-\frac{\mathsf{d_c}}{\ell'}\right)\right)\sigma_c,$$

but since $\ell' > \ell$, $\sigma^\infty < \sigma_D$ which is a contradiction. In other words, once σ_∞ has reached the critical value σ_D, one must decrease the loading if one wants to control the advance of the crack.

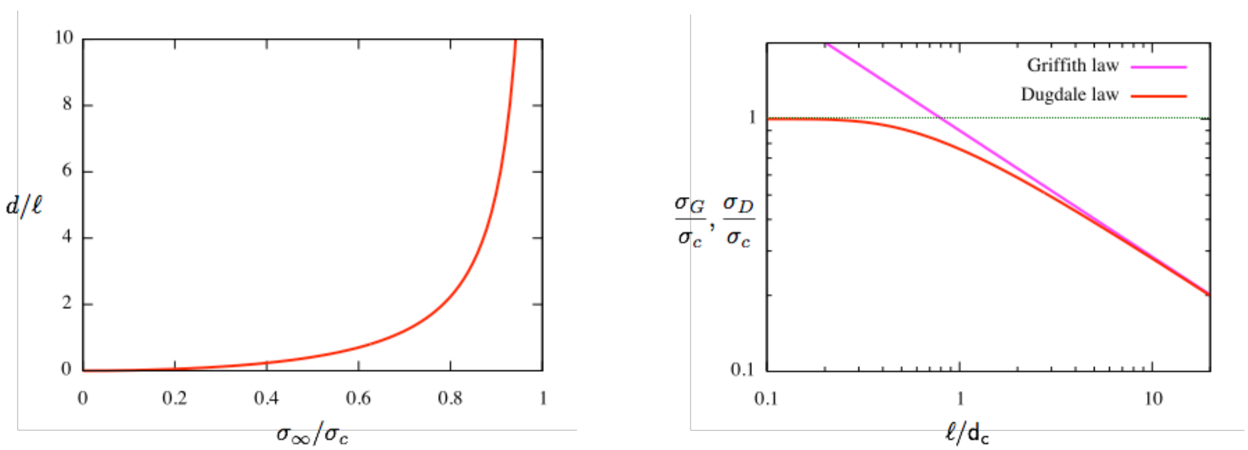

Figure 6: Left: dependence of the length of the cohesive crack on the loading. Right: Dependence of the maximal loading on the size of the initial cut for Griffith and Dugdale laws in a log-log diagram.

Let us compare the prediction of Dugdale's law concerning the maximal loading that the medium can sustain with that of Griffith's law. The graphs of σ_G and σ_D versus the length ℓ of the cut are shown in figure 6. First, one immediately sees in (23) or on the graph that σ_D is less than the maximal tension σ_c that the material can sustain, while σ_G goes to infinity when ℓ goes to 0. Moreover σ_D is close to σ_c when the length of the cut is small by comparison with the characteristic length $\mathsf{d_c}$ of the material. Thus, at small scales, Dugdale's law corrects the bad prediction of Griffith's law and the critical stress plays an essential role. On the other hand, when the ratio $\ell/\mathsf{d_c}$ is large, then the expansion of the expression of σ_D given in (23) with respect to the small parameter $\mathsf{d_c}/\ell$ gives at the first order

$$\sigma_D \approx \frac{2}{\pi}\sqrt{\frac{2\mathsf{d_c}}{\ell}}\sigma_c = \sigma_G.$$

That can be seen also on the graphs. Therefore, both laws give the same size effects at large scale and only $\mathsf{G_c}$ plays a role. The length which fixes the scales is $\mathsf{d_c}$ and not the critical opening δ_c. In practice, the ratio E/σ_c being large for a large class of materials, $\mathsf{d_c}$ is much greater than δ_c.

4.2. Nucleation of a "true" crack at the tip of a notch

In Section 3, we have obtained a local stress criterion for the nucleation of a cohesive crack in a body. Here we are interested by the next stage in the failure scenario: we want to find when and how a crack which in the first phase is entirely cohesive becomes a "true" crack in the sense that it contains a large part which is non-cohesive. This question will be studied in the case where the body contains a sharp notch, case which is both usual and important for an engineer. However to simplify the calculations, the problem is treated in the anti-plane setting. Specifically, we consider a two-dimensional sample like that of figure 7 which contains a notch whose angle is $\omega \in (\pi, 2\pi)$. (The limit value $\omega = 2\pi$ corresponds to a crack like in the example of the previous subsection, whereas the other limit value $\omega = \pi$ corresponds to a straight boundary. It turns out that the calculations that we will make remain valid when one passes to the limit of these two values of ω, but to simplify the presentation one considers that ω is in the open interval.) There are no body forces, the sides of the notch are free and another part of the boundary part is fixed, whereas the complementary part of the boundary is subjected to a distribution of anti-plane forces $tF\mathbf{e}_3$ proportional to the loading parameter t which grows from 0. The body is homogeneous and made of an isotropic material whose shear modulus is μ, and the evolution of the cracks is governed by Dugdale's law with τ_c as the maximal shear that the material can sustain.

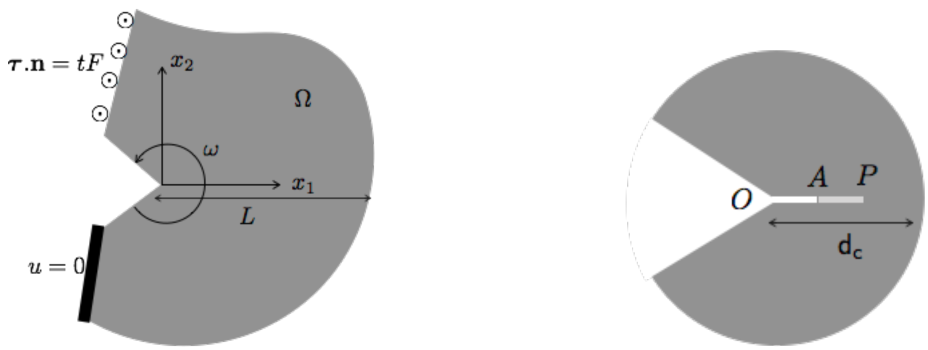

Figure 7: Left: the transverse section Ω of a body in an antiplane situation with a sharp notch of angle ω and a loading whose intensity is proportional to the parameter t. Right: a zoom of the tip of the notch with a nucleated crack along the axis of symmetry, OA and AP are respectively the non-cohesive and cohesive parts of the crack.

Accordingly, the displacement and the stress fields are of the form

$$\mathbf{u}(\mathbf{x}) = u(x_1, x_2)\mathbf{e}_3, \quad \boldsymbol{\sigma}(\mathbf{x}) = \tau_1(x_1, x_2)\mathbf{e}_1 \otimes_s \mathbf{e}_3 + \tau_2(x_1, x_2)\mathbf{e}_2 \otimes_s \mathbf{e}_3,$$

and $\boldsymbol{\tau}$ will denote the vector (τ_1, τ_2). The cohesive law reads as

$$\boldsymbol{\tau} \cdot \mathbf{n} \begin{cases} \in [-\tau_c, \tau_c] & \text{if} \quad [\![u]\!] = 0 \\ = \operatorname{sign}([\![u]\!])\tau_c & \text{if} \quad 0 < |[\![u]\!]| < \delta_c \ , \\ = 0 & \text{if} \quad |[\![u]\!]| > \delta_c \end{cases} \qquad \delta_c = \frac{\mathsf{G_c}}{\tau_c}.$$

Moreover, let us introduce the characteristic length of the material $\mathsf{d_c}$,

$$\mathsf{d_c} = \frac{\mu}{\tau_c}\delta_c = \frac{\mathsf{G_c}\mu}{\tau_c^2}.$$

We assume that $\mathsf{d_c}$ is small in comparison with the characteristic length L of the body Ω. This hypothesis will allow us to treat the problem by a two-scale approach, which is presented hereafter in an intuitive way.

- *The outer problem and its singularity.* As soon as the loading parameter t is not 0, a cohesive crack will appear at the tip of the notch because of the singularity of the elastic response. But, at the beginning, the length of the cohesive crack will be of the order of $\mathsf{d_c}$ and hence small by comparison with L. Consequently, from a macroscopic point of view, one can neglect in a first approximation that cohesive crack and consider that the response is purely elastic. That leads to the so-called outer problem where the presence of the crack is ignored. The displacement field solution of this elastic problem at "time" t, denoted u_t^e, is singular near the notch tip with a singular part which reads as

$$u_t^e(\mathbf{x}) = \mathsf{K}_t L \left(\frac{r}{L}\right)^{\frac{\pi}{\omega}} \sin\frac{\pi}{\omega}\theta + \cdots, \tag{24}$$

where L is taken as the reference length, (r, θ) denotes the polar coordinates $(x_1 = r\cos\theta, x_2 = r\sin\theta)$ and K_t is the dimensionless generalised stress intensity factor whose value depends on the geometry, the loading and the material parameters. However the dependence of K_t on t is linear and hence can read as

$$\mathsf{K}_t = t\bar{\mathsf{K}} \tag{25}$$

where $\bar{\mathsf{K}}$ is the value of the stress intensity factor for a loading parameter unity. We assume henceforth, that $\bar{\mathsf{K}}$ has been computed and is known.

- *The inner problem and its behaviour at infinity.* Let us now take d_c as the reference length and consider the problem near the crack tip. Since d_c/L is small, one can consider that the inner problem can be posed on the infinite angular sector $\mathcal{D}$:

$$\mathcal{D} = \{\mathbf{x} : x_1 = r\cos\theta, x_2 = r\sin\theta, r \in (0, +\infty), \theta \in (-\omega/2, +\omega/2)\}. \tag{26}$$

Of course, at this scale, the field u^e given by (24) cannot be the solution. But, since the crack is located near the notch tip and its length is of the order of d_c, one can assume that, far enough from the notch tip, u^e will be again a good approximation of the solution. That leads to consider that, in the first approximation, the behaviour at infinity of the displacement field is given by the singular part of u^e. Specifically, if one denotes by u^i the inner approximation of the displacement field, u^i which is defined on $\mathcal{D}$ must satisfy the following condition at infinity:

$$u^i(\mathbf{x}) \sim \mathsf{k}\delta_c \left(\frac{r}{\mathsf{d}_\mathsf{c}}\right)^{\frac{\pi}{\omega}} \sin\frac{\pi}{\omega}\theta \quad \text{when} \quad \frac{r}{\mathsf{d}_\mathsf{c}} \to +\infty. \tag{27}$$

Let us note that we choose a different normalisation for the stress intensity factor. Since $u^e_t(\mathbf{x})$ and $u^i(\mathbf{x})$ are both good approximations of the true displacement fields when r/L is small and r/d_c is large, respectively, comparing (24) and (27) gives the following relation between k and K_t:

$$\mathsf{K}_t = \mathsf{k}\frac{\tau_c}{\mu}\left(\frac{\mathsf{d}_\mathsf{c}}{L}\right)^{1-\frac{\pi}{\omega}}. \tag{28}$$

The renormalised stress intensity factor k will be used as the loading parameter for the inner problem. Thus, after this separation of scale, the inner problem becomes independent of the outer one because even the behaviour at infinity is characterised by the notch alone and not by the whole body and its loading. Therefore, since the behaviour at infinity of u^i is skew-symmetric in θ, we can assume that, by symmetry, the crack will appear and propagates along the axis $\theta = 0$, even if the body and its loading are not symmetric. (Of course, this is true only because we are interested in the first phase of the cracking, when the length of the crack is of the order of d_c.) So it remains to find the position ℓ of the tip of the non-cohesive crack and the size d of the cohesive crack in front of it as a function of k. This inner problem can be solved once for all, independently of the outer problem, the unique parameter being the notch angle ω (and the material constants μ, G_c and τ_c). The solution of the inner problem is given in Appendix A and we will use the results to answer to the question concerning when and how a non-cohesive crack appears.

With the help of the calculations made in Appendix A, the scenario of the evolution of the crack at the tip of the notch is the following:

1. As soon as k is not 0 and as long as it is small enough, a cohesive crack appears and propagate along the axis $\theta = 0$. Its length d is given as a function of k by

$$\left(\frac{d}{\mathsf{d}_\mathsf{c}}\right)^{1-\frac{\pi}{\omega}} = \frac{\pi^2\mathsf{k}}{2\omega\int_0^{\pi/2}(\sin\alpha)^{\frac{\omega}{\pi}-1}d\alpha}. \tag{29}$$

At the same time, the jump of u^i at 0 grows and reaches the critical value δ_c when k reaches k_D given by (48)-(49). The dependence of k_D on ω is weak as one can see on Figure 8. Specifically, $\mathsf{k}_D = 1$ when $\omega = \pi$, $\mathsf{k}_D = 2/\sqrt{\pi}$ when $\omega = 2\pi$ (this value is not the classical one because of our choice of normalisation of the stress intensity factor), the maximal value is around 1.28 for ω around $4\pi/3$.

2. After the onset of the non-cohesive crack, it is possible to find a solution of the inner problem but only by parametrising the response by the parameter $\alpha_m = \arcsin\left(\frac{\ell}{\ell+d}\right)^{\frac{\pi}{\omega}}$. The parametrised curve $\Big((\ell + d)(\alpha_m), \mathsf{k}(\alpha_m)\Big)$, with α_m growing from 0, is represented with dash-lines in the figure 9 for different values of ω. It turns out that k is always decreasing, except for the case $\omega = 2\pi$ where it remains constant. One can even see that the curve contains a snap-back when ω is greater than $7\pi/4$, and the closer ω to π the more pronounced the snap-back. This means that k_D is a limit load and that the propagation of the non-cohesive crack will be brutal just after its nucleation. It is not possible to find the length of the crack after this phase of brutal propagation (at least with the present two scale approach), and this so for several reasons: (i) the final length is not of the order of d_c because

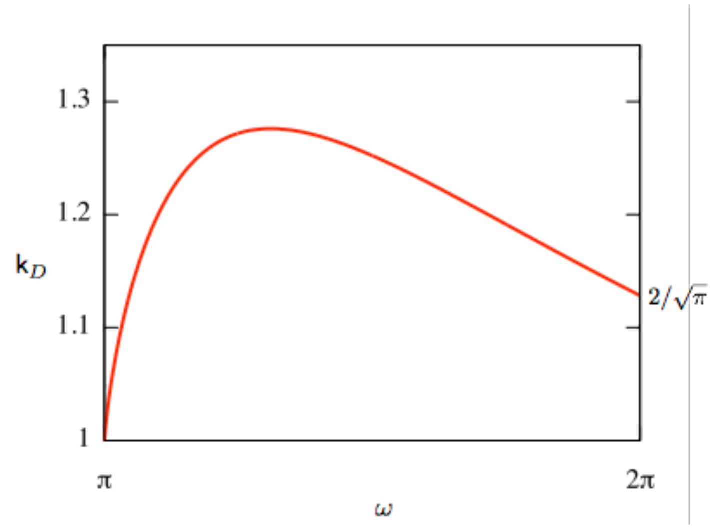

Figure 8: Critical value of the renormalised stress intensity factor at which a non-cohesive crack appears vs the angle of the notch.

there is no solution at this scale with $\mathsf{k} > \mathsf{k}_D$; (ii) the discontinuity of the evolution of the crack requires to introduce a new criterion to find the final value of the crack length and the choice of that criterion is debatable; (iii) it is not clear if one can remain in the quasi-static setting and neglect inertial effects during this unstable phase of propagation. In conclusion, the answer to the question of *when* the "true" crack appears has been found, but the question of *how long* is its initiated length remains open.

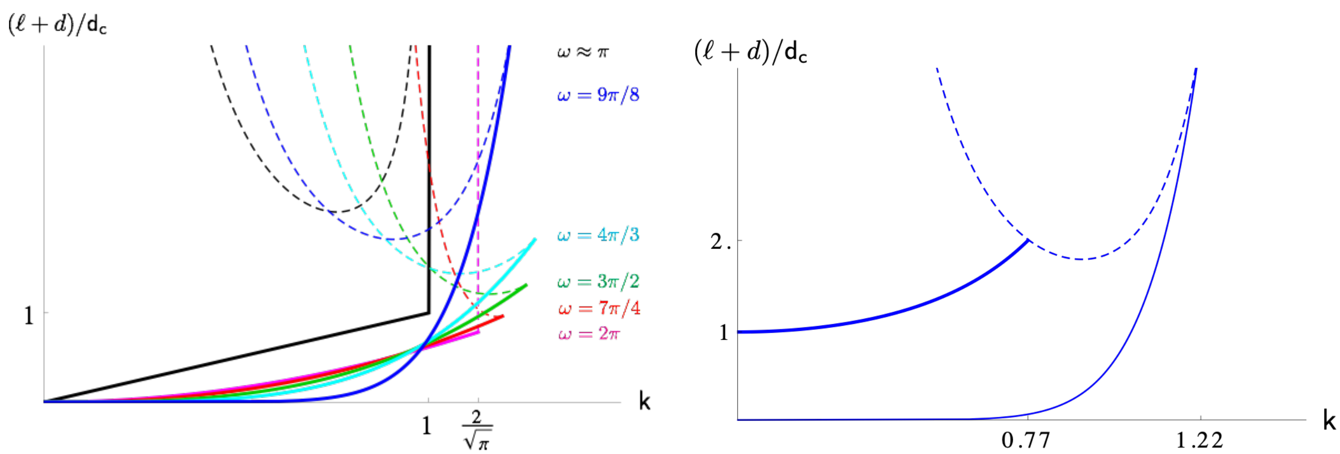

Figure 9: Left: Evolution of the tip of the crack for different values of the notch angle. The solid lines represent the length of the cohesive crack vs the stress intensity factor before the nucleation of a non-cohesive crack; the limit points correspond to the onset of the non-cohesive crack. The dashed lines represent the evolution after the nucleation by assuming that the ratio $\ell/(\ell + d)$ between the length of the non-cohesive part of the crack over the total length of the crack can be controlled; this requires decreasing the loading, otherwise the propagation of the crack is unstable. Right: Case of a preexisting crack of initial length $\mathsf{d_c}$. The thick line curve represents the evolution of the cohesive crack tip ahead the initial crack. When this curve crosses the dashed curve, the initial crack propagates. The angle of the notch is $9\pi/8$.

Note however that, even though the response given by the dashed curve for the crack propagation cannot be directly observed, this curve plays an important role in presence of an imperfection. Indeed, let us assume that there exists at the tip of the notch an initial non-cohesive crack whose length ℓ_0 is of the order of $\mathsf{d_c}$. Then, during a first phase, the initial crack does not propagate but a non-cohesive crack appears in front of its tip, whose size d increases when k increases. The corresponding response, characterised by the dependence of $\ell_0 + d$ on k, can still be calculated using the equations (44), (45) and (47) of Appendix A. (Actually the curve is also parameterised by α_m, but now α_m starts from $\pi/2$ and decreases). Therefore, when the curve of that response intersects the curve in dashed line, the jump of the displacement at the tip of the initial crack is exactly equal to δ_c (and the two parameters α_m are equal). Hence, the initial crack will propagates at the value of k corresponding to the point of intersection which is smaller than k_D. For example, when $\omega = 9\pi/8$ and $\ell_0 = \mathsf{d_c}$, then the initial crack will propagate at $\mathsf{k} \approx 0.77$ whereas $\mathsf{k}_D \approx 1.22$, which corresponds to a loss of about 37% on the load of initiation of a macro-crack.

To conclude this section, let us return to the problem posed on the whole body. The critical stress intensity factor k_D at which a non-cohesive crack appears at the tip of a notch is now known and depends only on the notch angle. Hence, inserting this value into (28) and using (25) gives the critical value of the loading t_D at which a non-cohesive crack appears at the tip of the notch:

$$t_D = \frac{\mathsf{k}_D}{|\bar{\mathsf{K}}|}\frac{\tau_c}{\mu}\left(\frac{\mathsf{d_c}}{L}\right)^{1-\dfrac{\pi}{\omega}}. \tag{30}$$

(The presence of the absolute value of $\bar{\mathsf{K}}$ in (30) comes from the fact all the calculations in the inner problem have been made with $\mathsf{k} > 0$. In reality k has the sign of $\bar{\mathsf{K}}$, but since the inner problem is symmetric if k is changed in $-\mathsf{k}$, there is no loss of generality and (30) holds in any case.) If the body contains several notches, this formula can be used for each notch because they do not interact during this phase of nucleation (except in the value of $\bar{\mathsf{K}}$ which is a global quantity). Then comparing all the critical values allows us to find at which notch a "true" crack will nucleate first. Since the inner problem has been solved once and for all, this requires only to solve an elastic problem posed on the whole body to find the value of $\bar{\mathsf{K}}$ at each notch.

5. Introduction of an irreversibility condition and fatigue effects

It is not possible to account for fatigue phenomena, *i.e.,* the propagation of a crack under cyclic loading, within Griffith's theory, because the response is unchanged after the first cycle. For this reason, specific laws have been developed by engineers to account for fatigue effects, the most used being Paris law Paris et al. (1961); Paris and Erdogan (1963), where the growth of the length of the crack during one cycle is given in terms of the amplitude of variation of the potential energy release rate during the cycle. Formally, the law reads as

$$\frac{d\ell}{dN} = f(\Delta G).$$

This formula is completely empirical, the parameters of the law are identified from specific experiments without a link was made with Griffith's law which remains valid under monotonic loading. The goal of this section is to show that it becomes possible to account for fatigue effects with a cohesive force model, and moreover, to construct from it a Paris-type fatigue law and to make the link with Griffith's law. However the price to pay is that this requires to introduce a "right" irreversibility condition into the cohesive force model. This step is the most delicate and debatable one because there exists an infinite number of possible choices, see for instance Yang et al. (1999); Nguyen et al. (2001); Roe and Siegmund (2002); Talon and Curnier (2003); Siegmund (2004); Abdul-Baqi et al. (2005); Maiti and Geubelle (2005) to cite a few, and we are only guided by phenomenological considerations.

5.1. The choice of the irreversibility condition and the changes induced in the cohesive law

It is essential that the cohesive forces depend on the sign of the rate of the displacement jump and not only on the current value of the displacement jump. Owing to this directional rate dependence, we obtain different responses during the loading and unloading phases. Moreover, by introducing into the constitutive relation a memory variable which cumulates all the oscillations of the displacement jump, one can explain that the cohesive forces decrease gradually to zero. Therefore, by this effect of accumulation under cyclic loading, all the liaisons will finally break everywhere along the crack path, even if the amplitude of the loading is small. The simplest way to include that effect into the cohesive law is to proceed as in plasticity where the cumulated plastic strain plays the role of an internal variable memorising all the history of the plastic strain. This cumulative variable enters in the definition of the dissipated energy instead of the current plastic strain.

Thus, let us consider the case where a cohesive crack is always in mode $\mathtt{I}$ in the sense that the normal displacement u_n only is discontinuous. Let us define the cumulated opening δ by

$$\dot{\delta} = \left(\llbracket \dot{u}_n \rrbracket\right)^+, \qquad \text{with} \qquad x^+ = \max\{x, 0\}, \tag{31}$$

and let us replace $\llbracket u_n \rrbracket$ by δ in the definition of the surface energy density associated with the model of Dugdale (of course, this can be done for any Barenblatt-type model). Then, $\Phi(\delta)$ will represent all the dissipated energy at a point of the crack during the entire history of its opening. Since δ can only increase, so will this energy. Hence, let us assume that this point is submitted to a cyclic loading during which the opening oscillates between 0 and a maximal value less than δ_c. After a certain number of cycles, δ becomes greater than δ_c and the surface energy density reaches the Griffith's value $\mathsf{G_c}$. Accordingly, the cohesive forces vanish for ever at this point. In other words, it is now possible to break the liaison simply by a cumulative effect, see Figure 10. The main criticism that can be made of this choice is that it is difficult to find a justification for it by a small-scale physical mechanism.

Since the definition of the surface energy has changed, one must also change the manner by which the cohesive forces are deduced. This can be done by a variational procedure and the interested reader is referred to Abdelmoula et al. (2010), but here we simply give

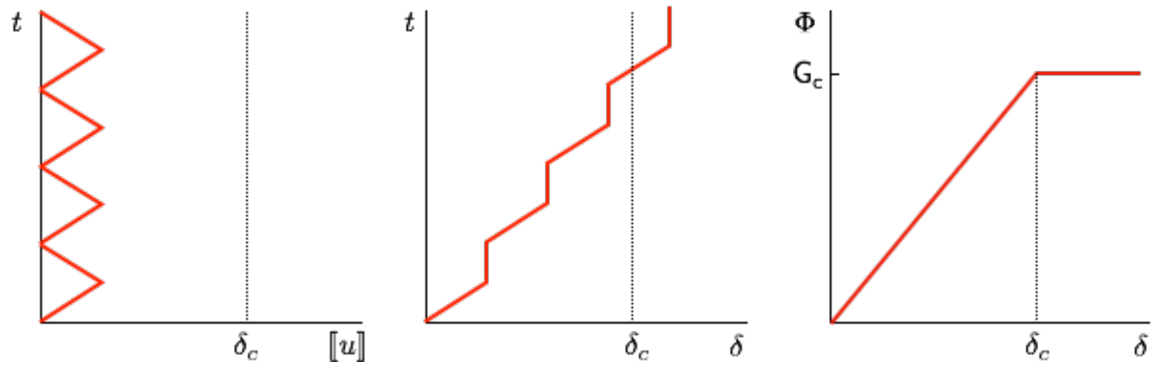

Figure 10: Illustration of the cumulative effect of a cycle with a small amplitude on the Dugdale surface energy density which depends now on the cumulative opening.

the result. Specifically, the new law governing the evolution of the cohesive forces reads as follows:

$$\text{(IR)}: \quad \dot{\delta} = \big([\![\dot{u}_n]\!]\big)^+, \qquad \text{(ST)}: \quad 0 \leq \sigma_{nn} \leq \Phi'(\delta), \qquad \text{(EB)}: \quad \sigma_{nn}[\![\dot{u}_n]\!] = \Phi'(\delta)\dot{\delta}. \tag{32}$$

In (32), (IR) is the definition of the cumulated opening which contains the irreversibility condition; (ST) is a stability condition which can be deduced from the new form of the surface energy density by proceeding as was done in Section 3 to obtain the yield stress criterion; (EB) is an energy balance which requires that the power expended by the normal stress through the opening rate be equal to the dissipated power on the surface. From (ST) one checks that the cohesive forces vanish as soon as $\delta > \delta_c$ because $\Phi'(\delta) = 0$. So, we have only to consider the case when $0 < \delta < \delta_c$. In this case, $\Phi'(\delta) = \sigma_c$ and we can distinguish three regimes according to the sign of $[\![\dot{u}_n]\!]$:

- *When* $[\![\dot{u}_n]\!] > 0$. Then $\dot{\delta} = [\![\dot{u}_n]\!] > 0$ and (EB) gives $\sigma_{nn} = \sigma_c$; the cohesive forces are *activated*.
- *When* $[\![\dot{u}_n]\!] < 0$. Then $\dot{\delta} = 0$ and (EB) gives $\sigma_{nn} = 0$; the cohesive forces are *passive*.
- *When* $[\![\dot{u}_n]\!] = 0$. Then σ_{nn} is in the interval $[0, \sigma_c]$ by (ST), but remains undetermined; it is the *neutral regime*.

Hence the cohesive forces essentially depend now on the sign of the opening rate: they are activated when the opening increases, they are passive when the opening decreases.

5.2. Construction of the fatigue law by a two-scale approach

The cohesive law with its irreversibility condition can be used for any type of loading, monotonic as well as cyclic, with a small number as well as a great number of cycles or more generally for any complex loading history. That constitutes a first major difference with Griffith's law or Paris' law whose use is reserved for specific conditions of loading. Here we will use it in the classical experiment consisting in the propagation of a crack in a Compact Test sample subjected to a cyclic loading.

5.2.1. Setting of the problem and main assumptions

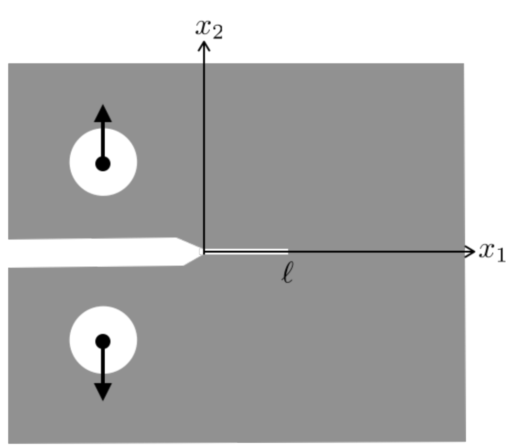

Figure 11: Compact Test sample with a crack of length ℓ created by fatigue under a cyclic loading.

Specifically, in plane strain, let us consider the body represented in Figure 11. The sample and the loading are symmetric so that the crack will propagate along the axis $x_2 = 0$ and will be always in mode I. The intensity of the applied forces oscillates between 0 and a maximal value F. We assume that after a (large) number of cycles, the tip of the crack is at $x_1 = \ell$ and we start the analysis from this situation.

First, we make the fundamental assumption that the characteristic length of the material $\mathsf{d_c}$, given in the plane-strain setting by

$$\mathsf{d_c} = \frac{\pi}{8(1-\nu^2)} \frac{\mathsf{EG_c}}{\sigma_c^2}, \tag{33}$$

is *small* in comparison with the characteristic dimensions of the sample and, in particular, with the crack length ℓ. That allows us to use a two-scale approach *both in space in time*, in the spirit of what is made in the previous section. Specifically, we make the *a priori* following assumptions that will be checked *a posteriori*:

(i) The width of the cohesive crack is at most of the order of $\mathsf{d_c}$;

(ii) The growth of the non-cohesive crack is at most of the order of $\mathsf{d_c}$ at each cycle.

This means that the number of cycles N needed to obtain a crack of length ℓ is at least of the order of $\ell/\mathsf{d_c}$ and, hence, large. Let us renumber the cycles starting from N and call $i = 0$ the last cycle which leads to the situation at which the discussion starts. The time is also rescaled in such a manner that $t = 0$ corresponds to the end of cycle $i = 0$ and the duration of a cycle is 1. Hence $t = i$ corresponds to the end of the cycle i and the start of the cycle $i + 1$.

From a macroscopic point of view, *i.e.,* at the scale of the sample, the cohesive part of the crack can be neglected and the growth of the crack also can be neglected during a few cycles before or after $i = 0$ (“a few” means small by comparison with N). Consequently, at the scale of the sample and for a few cycles, the problem is an elastic problem posed in a body which contains a non propagating crack and is submitted to the cyclic loading. The solution is singular at the tip of the crack with a singularity corresponding to the mode I. The stress intensity factor oscillates between 0 and the maximal value $\mathsf{K_I}$ corresponding to the maximal value of the applied force. Of course, $\mathsf{K_I}$ depends on ℓ, but, since the growth of the crack is neglected, it is considered as fix for a few cycles.

5.2.2. The inner problem, its solving and the getting of the fatigue law

Now let us take d_c as the reference length and consider the problem near the crack tip. As in the previous section, the inner problem is posed on the whole plane with the singularity of the outer problem as behaviour at infinity. The value of the stress intensity factor at time t, say $\mathsf{K_I}(t)$, will act as the loading parameter. The dependence of $\mathsf{K_I}(t)$ on t is periodic, decreasing from $\mathsf{K_I}$ to 0 during the first half of the cycle i , then increasing from 0 to $\mathsf{K_I}$ during the second half. We seek a stationary regime for the evolution of the crack cycle

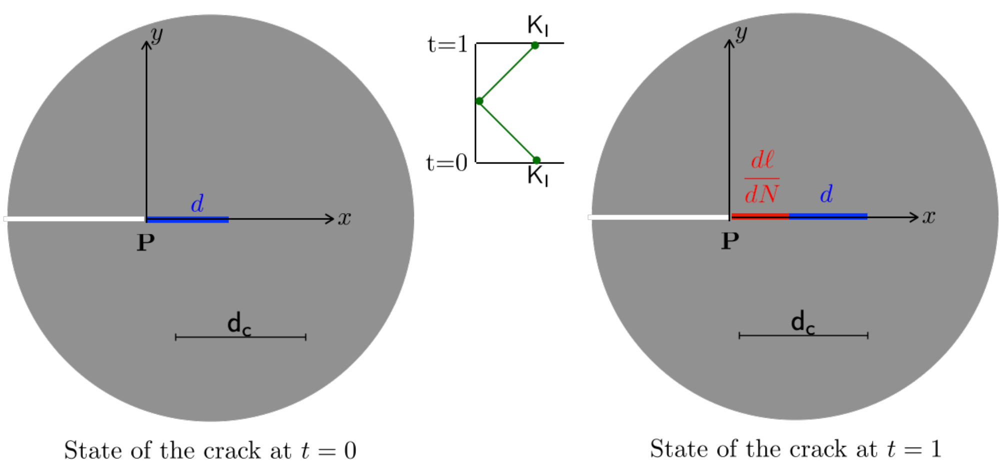

Figure 12: State of the crack near the tip of the non-cohesive crack just at the start of the cycle $i = 1$ (left) and just at the end of that cycle (right); in blue the cohesive zone of width d, in red the growth of the non-cohesive crack during the cycle. Using the rescaled time t, the duration of a cycle is 1 and the cycle $i = 1$ corresponds to $t \in (0, 1)$. During a cycle, the stress intensity factor is first decreasing from $\mathsf{K_I}$ to 0, then increasing from 0 to $\mathsf{K_I}$.

after cycle. This means that we are looking for an evolution where the growth of the crack $d\ell/dN$ is the same at each cycle, and where the dependence on time of the displacement field, the stress field and the cumulated opening field is as follows:

$$\mathbf{u}^t(x,y) = \mathbf{u}^{t-1}\big(x - \frac{d\ell}{dN}, y\big), \quad \boldsymbol{\sigma}^t(x,y) = \boldsymbol{\sigma}^{t-1}\big(x - \frac{d\ell}{dN}, y\big), \quad \delta^t(x) = \delta^{t-1}\big(x - \frac{d\ell}{dN}\big), \tag{34}$$

where the superscript denotes the time at which the field is considered. Of course, these relations must hold for all t. In other words, the same fields are reproduced cycle after cycle with only a shift of $d\ell/dN$ in space in the direction of propagation. The ultimate goal is to determine $d\ell/dN$, its relation with K_I constituting the searched fatigue law.

The determination of the solution and the achievement of this goal requires a careful analysis of the evolution of the cohesive zone during one cycle. The most difficult task is to find the parts in which the cohesive forces are active, passive or neutral, respectively. For this purpose, one must use the generic problem treated in Appendix B which gives the solution of the elastic problem corresponding to a given stress intensity factor as loading at infinity and a given distribution of the cohesive forces on the crack lips. Here we simply show qualitatively in Figure 13 the different phases of the evolution of the cohesive zone during a cycle, the reader interested by a complete proof must refer to Abdelmoula et al. (2010). Let us comment these different phases:

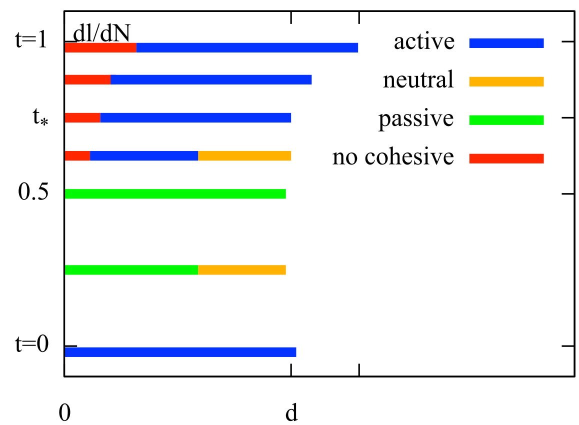

Figure 13: Evolution of the cohesive zone with its different regimes during one cycle.

1. At the end of the previous cycle $i = 0$, all the cohesive zone was active, the opening rate being positive everywhere;
2. During the unloading a part of the cohesive zone, ahead the tip of the non-cohesive crack, is passive and the other part is neutral. The cumulated opening, the tips of the cohesive crack and of the non-cohesive crack do not evolve. The passive zone progressively grows.
3. At the end of the unloading ($t = 0.5$), all the cohesive zone is passive and the displacement field vanishes.
4. As soon as the stress intensity factor increases, the opening rate becomes positive ahead the tip of the non-cohesive crack, hence the cumulated opening increases and becomes larger than δ_c (because $\delta^0(0) = \delta_c$ by definition of the tip of the non-cohesive crack). Hence, *the non-cohesive crack will continuously grow until the end of the cycle*.
5. During a first phase of the reloading, only a part of the cohesive crack is active, the other part is neutral. Therefore the tip of the non-cohesive crack does not propagate.
6. At time t_* all the cohesive zone is active. After t_* both ends evolve and all the cohesive crack is active;
7. At the end of the cycle, the length of the non-cohesive crack has increased of $d\ell/dN$ and the length of the cohesive zone is the same as at the beginning of the cycle.

An important fact is that during all the unloading phase $\dot\delta = 0$ everywhere, whereas during all the reloading phase $[\![\dot u_2]\!] \geq 0$ everywhere. This will allows us to calculate $d\ell/dN$ without having to know all the details of the evolution during the different phases (but of course it was necessary to solve all the problem to prove the properties shown before). Indeed, by definition of the cumulated opening and by virtue of the properties already obtained, one has for $x \in [0, d]$:

$$\delta^0(x) - \delta^{-1}(x) = \int_{-1}^{0} \left([\![\dot u_2^t]\!](x)\right)^+ dt = \int_{-1/2}^{0} [\![\dot u_2^t]\!](x)dt = [\![u_2^0]\!](x) - [\![u_2^{-1/2}]\!](x) = [\![u_2^0]\!](x),$$

where the last equality is due to the vanishing of the displacements at the end of the unloading. Repeating this calculation for the cycle $i = -1$ and using the stationarity condition (34) gives

$$\delta^0(x) - \delta^{-2}(x) = [\![u_2^0]\!](x) + [\![u_2^{-1}]\!](x) = [\![u_2^0]\!](x) + [\![u_2^0]\!]\big(x + \frac{d\ell}{dN}\big).$$

Hence by induction, since δ^{-n} vanishes on $[0,d]$ for n large enough, one gets

$$\delta^0(x) = \sum_{i=0}^{\infty} [\![u_2^0]\!]\big(x + i\frac{d\ell}{dN}\big),$$

where we consider an infinite sum because the number of cycles involved in the calculation of δ^0 is not known at this stage. The cumulated opening at the tip of the non-cohesive crack being equal to δ_c, one has $\delta^0(0) = \delta_c$ which leads to

$$\sum_{i=0}^{\infty} [\![u_2^0]\!]\big(i\frac{d\ell}{dN}\big) = \delta_c. \tag{35}$$

It remains to determine d and $[\![u_2^0]\!](x)$ for $x \in [0,d]$ to obtain the equation for $d\ell/dN$. At $t=0$, the tip of the non-cohesive crack is at $x=0$, the length of the cohesive zone is d (to be determined), all the cohesive zone is active and the stress intensity factor is $\mathsf{K_I}$. Hence $\mathbf{u}^0$ is solution of the generic problem treated in Appendix B with $\mathsf{L}=0$, $\mathsf{D}=d$ and $\mathsf{K}=\mathsf{K_I}$. Accordingly, d is obtained by requiring that there is no singularity at the tip of the non-cohesive crack and hence is given by (54):

$$d = \frac{\mathsf{G}}{\mathsf{G_c}}\mathsf{d_c} \quad \text{with} \quad \mathsf{G} = (1-\nu^2)\frac{\mathsf{K_I}^2}{\mathsf{E}}. \tag{36}$$

In (36) G is the energy release rate given by Irwin's formula in terms of the stress intensity factor $\mathsf{K_I}$. Moreover, $[\![u_2^0]\!]$ is given by (57) and reads here

$$[\![u_2^0]\!](x) = V\Big(\frac{x}{\mathsf{d_c}}\frac{\mathsf{G_c}}{\mathsf{G}}\Big)\frac{\mathsf{G}}{\mathsf{G_c}}\delta_c \tag{37}$$

where $V(\zeta)$ is defined for $\zeta \geq 0$ by (see also its graph in figure 17):

$$V(\zeta) = \begin{cases} 1 & \text{if } \zeta = 0, \\ \sqrt{1-\zeta} - \zeta\ln(1+\sqrt{1-\zeta}) + \zeta\ln\sqrt{|\zeta|} & \text{if } 0<\zeta<1, \\ 0 & \text{if } \zeta \geq 1. \end{cases} \tag{38}$$

Finally, inserting (37) into (35) gives the desired equation for the growth $d\ell/dN$ of the crack at each cycle:

$$\boxed{\sum_{i=0}^{\infty} V\left(\frac{i}{\mathsf{d_c}}\frac{d\ell}{dN}\frac{\mathsf{G_c}}{\mathsf{G}}\right)\frac{\mathsf{G}}{\mathsf{G_c}} = 1.} \tag{39}$$

The study of this equation is the object of the next subsection.

5.2.3. *Properties of the fatigue law and checking of the* a priori *hypotheses*

Let us first analyse here the conditions for the existence and the uniqueness of a solution of (39) for $d\ell/dN$ according to the value of G. One gets the following properties (here below $\dot\ell$ stands for $d\ell/dN$):

1. *If* $\mathsf{G} > \mathsf{G_c}$, *then there exists no solution for* $\dot\ell$.

   Indeed, since $V \geq 0$ and $V(0)=1$, $\sum_{i=0}^{+\infty} V\big(\frac{i\dot\ell\mathsf{G_c}}{\mathsf{d_c}\mathsf{G}}\big)\frac{\mathsf{G}}{\mathsf{G_c}} \geq V(0)\frac{\mathsf{G}}{\mathsf{G_c}} > 1$ for all $\dot\ell$.

2. *If* $\mathsf{G} = \mathsf{G_c}$, *then all the* $\dot\ell$ *greater than or equal to* $\mathsf{d_c}$ *are solutions.*

   Indeed, in such a case, (39) becomes $\sum_{i=0}^{+\infty} V\big(i\dot\ell/\mathsf{d_c}\big) = 1$. Since $V(0)=1$, it reads also as $\sum_{i=1}^{+\infty} V\big(i\dot\ell/\mathsf{d_c}\big) = 0$. But since $V(\zeta)$ is non negative and vanishes if and only if $\zeta \geq 1$, the result follows.

3. *If* $0 < \mathsf{G} < \mathsf{G_c}$, *then there exists a unique solution which can read as* $\dot\ell = \mathsf{f}(\mathsf{G}/\mathsf{G_c})\mathsf{d_c} > 0$.

   Indeed, let us consider the function $\lambda \mapsto F(\lambda) := \sum_{i=0}^{+\infty} V\big(i\lambda/d\big)\mathsf{G}$ with $d = \mathsf{d_c}\mathsf{G}/\mathsf{G_c}$. Since $V(0)=1$, then $F(0)=+\infty$. Since $V(\zeta)=0$ for $\zeta \geq 1$, then $F(\lambda) = \mathsf{G} < \mathsf{G_c}$ for every $\lambda \geq d$. When $0<\lambda<d$, since V is decreasing on $[0,1]$ and vanishes on $[1,+\infty)$, then $F(\lambda)$ is decreasing. Hence F decreases from infinity to G as λ goes from 0 to d. Therefore, there exists a unique $\dot\ell$ such that $F(\dot\ell) = \mathsf{G_c}$. Moreover, $\dot\ell \in (0,d)$.

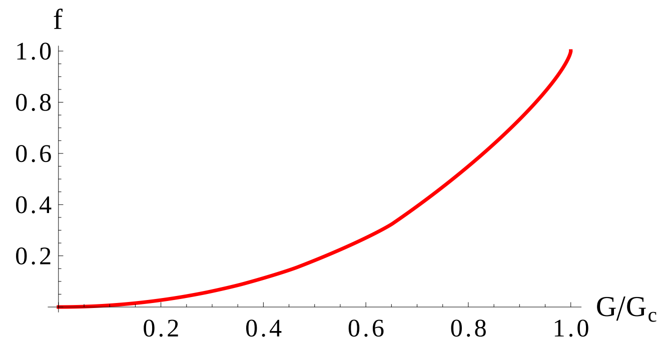

Figure 14: *Graph of the function* f *giving the fatigue law*

The first two properties are in agreement with Griffith's law: the energy release rate cannot be greater than $\mathsf{G_c}$ and the growth rate of the crack is undetermined when the energy release rate is equal to $\mathsf{G_c}$. On the other hand, if the energy release rate at the end of the loading phase of a cycle is less than $\mathsf{G_c}$, then the crack propagates progressively from one cycle to the other (whereas there is no propagation with Griffith's law). The presence of this subcritical regime is due to the introduction of cohesive forces and of the cumulated opening concept into the model.

The graph of f is plotted in figure 14 and one sees that $\mathsf{f}(g)$ is monotonically increasing from 0 to 1 when $\mathsf{G}/\mathsf{G_c}$ grows from 0 to 1. Let us establish an additional property for the function f.

Property 4. *For small values of* $g = \mathsf{G}/\mathsf{G_c}$*, we have* $\mathsf{f}(g) = g^2/3 + o(g^2)$ *and the fatigue law is like a Paris' law with exponent 2 in terms of the energy release rate and hence with exponent 4 in terms of the stress intensity factor:*

$$\frac{d\ell}{dN} \approx \left(\frac{\mathsf{G}}{\mathsf{G_c}}\right)^2 \frac{\mathsf{d_c}}{3}. \tag{40}$$

Let us prove this property. Let us set $n(g)$ the greatest i which gives a non-zero contribution in the calculation of the sum in (39). Since $V(\zeta)$ vanishes as soon as $\zeta \geq 1$, $n(g)$ is the integer part of $g/\mathsf{f}(g)$. Since $\sum_{i=0}^{n(g)} gV(i\mathsf{f}(g)/g) = 1$ and V is less than 1, necessarily $\lim_{g\to 0} n(g) = +\infty$. Hence $\lim_{g\to 0} n(g)\mathsf{f}(g)/g = 1$. Therefore,

$$\lim_{g\to 0} \frac{\mathsf{f}(g)}{g^2} = \lim_{g\to 0} \sum_{i=0}^{n(g)} \frac{1}{n(g)} V\left(\frac{i}{n(g)}\right) = \int_0^1 V(\zeta)d\zeta = \frac{1}{3},$$

and the result follows. Note that the number of cycles $n(g)$ involved in the calculation of the sum in (39) is of the order of $1/g$ and hence large when g is small. But in turn $d/\mathsf{d_c}$ is of the order of g and $\dot{\ell}/\mathsf{d_c}$ of the order of g^2. That means that if g remains small all along the propagation of the crack, then the number N of cycles needed to obtain a crack of length ℓ will be of the order of $g^{-2}\ell/\mathsf{d_c}$ and hence very large by comparison with $n(g)$.

Finally, let us check *a posteriori* whether the hypotheses made *a priori* to construct the fatigue law are really satisfied. Of course, when G is greater than $\mathsf{G_c}$, the propagation of the crack is unstable and the fatigue law is meaningless. The case $\mathsf{G} = \mathsf{G_c}$ also cannot be covered by a fatigue law. So, let us consider the case when $\mathsf{G} < \mathsf{G_c}$. We have found that the size of the cohesive zone and the growth of the non-cohesive crack are always of the order of $\mathsf{d_c}$ and hence both are small by comparison with ℓ as expected.

5.2.4. Concluding remarks on the fatigue law

The construction of the fatigue law is based on a separation of scales in space and time which is valid provided that the characteristic length of the material is small by comparison with any characteristic length of the body. The small-scale problem consists of determining the stationary regime governing the evolution of the crack and of the cohesive zone during one cycle of loading with the stress intensity factor as the loading parameter. This problem has a universal character since it does not depend on the geometry of the body, the crack path or the boundary conditions. Therefore, the resulting fatigue law is characteristic of the material properties (including its bulk behaviour and the cohesive model) for a given type of cyclic loading. But of course the fatigue law depends on the choice of the surface energy density, on the choice of the memory variable, and, more generally, on the irreversibility condition and the type of cyclic loading. In the case of a linear elastic material with a Dugdale-type surface energy depending only on the cumulated opening, we have obtained (for simple unloading-reloading cycles) a Paris-type fatigue law which is approximatively a power law like $d\ell/dN = C\mathsf{K_I}^4$ for small values of $\mathsf{K_I}$. An interesting task will be to understand the origin of the exponent 4 or to obtain other exponents by changing the surface energy, the loading-unloading conditions and the bulk behaviour of the material. Some partial results are available in Abdelmoula et al. (2009, 2010), but the essential remains to be done.

6. Conclusion

As we have shown all along the paper, the reintroduction of an interaction between the lips of a crack which is ignored in Griffith's theory can change radically the evolution of the crack even if this interaction is confined near the crack tip. As the cohesive models introduce a critical stress and an internal length, it becomes possible to model the nucleation of a crack in a sound body and to account for realistic size effects. Moreover, after the introduction of a pertinent irreversibility condition, it becomes possible to model fatigue effects. Symmetrically, under monotonic loading and once the size of the crack is large in comparison to the internal length of the material, the propagation of the crack predicted by the cohesive force models is practically the same as in Griffith's theory. In other words, this reintroduction of the interaction between the lips corrects the predictions of Griffith's theory when it is necessary, but does not change substantially the response when it is not necessary.

Moreover, if one refines the analysis, it appears that the predictions of the cohesive force models allow us to make a link with some laws empirically introduced to account for a particular phenomenon concerning the failure of materials or engineering structures. It is the case for the nucleation of crack where one recovers the usual criteria of strength of materials simply by using a stability criterion and an isotropy assumption. It is also the case for fatigue effects where one recovers empirical fatigue laws simply by using a two-scale approach and a cohesive force model with an irreversibility condition.

Comparatively with other approaches like gradient damage models which contains the same ingredients as a critical stress and an internal length and which are also (partially) able to correct the main defects of Griffith's theory, the cohesive models have the great advantage to be construct on a solid physical basis. In consequence, their under-employment is probably due to their difficulty of implementation, in contrast with gradient damage models. Specifically, we can identify the two following main issues with the use of cohesive models.

The mathematical issue. The first issue has a theoretical character and concerns the existence of "classical" solutions. Indeed, if we consider the energy functional introduced in Section 3, see (4), it has bad mathematical properties because it is not lower semi-continuous. That means that, if we try to minimise the energy by constructing a minimising sequence $\mathbf{u}_n$, this sequence will not converge in general to a classical $\mathbf{u}$ with a jump set on one hand and a regular part on the other hand. The physical interpretation of this fact is that the material will develop fine mixtures of elastic zones and cracks with micro-jumps in order to minimise the energy. (Note that this phenomenon does not exist in Griffith's theory because the price to pay in terms of surface energy is too high.) Consequently, those cracks finely embedded in the material change the behaviour *in the bulk* and not only on isolated surfaces of discontinuities. To find this effective behaviour in the bulk is a really difficult problem: it is not only a classical problem of homogenisation which consists in finding the effective behaviour of a given microstructure, but it is also necessary to find the optimal microstructure. This task has been achieved in the restricted context of anti-plane displacements without an irreversibility condition Bouchitté et al. (1995); Braides et al. (2001); Dal Maso and Garroni (2008). Practically nothing is known in the three-dimensional case with irreversibility.

The numerical issue. The second issue concerns the practical management of free discontinuity surfaces. In Griffith's theory the same difficulty exists and is overcome by regularisation of the energy: it is partially the role of gradient damage models. Thus, the challenge is to adapt these regularisation methods to the case of cohesive force models. Some results have been obtained in that direction Conti et al. (2016), but the problem remains essentially open.

These issues constitute very exciting challenges from a research point of view. Hence, there is no reason not to continue exploring this path.

A. Resolution of the inner problem at the tip of a notch

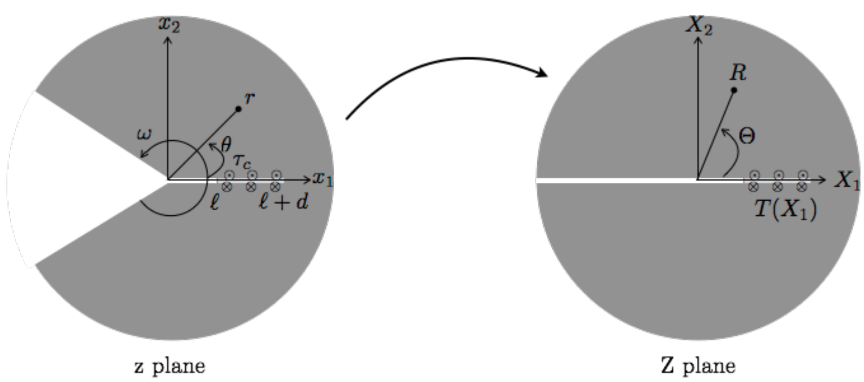

Figure 15: Transformation of the infinite angular sector into a plane with a cut.

Let us consider the infinite angular sector $\mathcal{D}$ defines in the polar coordinates system as $r \in (0, +\infty)$ and $\theta \in (-\omega/2, +\omega/2)$ with $\omega \in (\pi, 2\pi]$, $\omega = \pi$ being excluded because several expressions obtained hereafter are not valid in that case. Let $\Gamma_0 = (0, \ell) \times \{0\}$, with

$\ell \geq 0$, be the non-cohesive part of the crack, let $\Gamma_c = (\ell, \ell+d) \times \{0\}$ with $d > 0$, be the cohesive part of the crack. Moreover let $\mathsf{k} > 0$ be the renormalised stress intensity factor. Then, at given ℓ, d and k, the anti-plane displacement field u^i and its associated stress field $\boldsymbol{\tau}^i = \mu \nabla u^i$ must satisfy

$$\begin{cases} \mathrm{div}\boldsymbol{\tau}^i = 0 & \text{in} \quad \mathcal{D} \setminus (\Gamma_0 \cup \Gamma_c) \\ \tau_2^i = 0 & \text{on} \quad \Gamma_0 \\ \tau_2^i = \tau_c & \text{on} \quad \Gamma_c \\ \tau_\theta = 0 & \text{at} \quad \theta = \pm\omega/2 \\ u^i \sim \mathsf{k}\delta_c \left(\dfrac{r}{\mathsf{d_c}}\right)^{\frac{\pi}{\omega}} \sin \frac{\pi}{\omega}\theta & \text{at infinity} \end{cases}$$

This problem can be solved in a closed form by using complex potentials, see Muskhelishvili (1963). Denoting $z = x_1 + \mathrm{i}x_2$ the complex variable, one considers the transform $z \mapsto Z = X_1 + \mathrm{i}X_2 = \mathsf{d_c}(\frac{z}{\mathsf{d_c}})^{\frac{2\pi}{\omega}}$ which transform (r, θ) into $(R, \Theta) = \left(\mathsf{d_c}(\frac{r}{\mathsf{d_c}})^{\frac{2\pi}{\omega}}, \frac{2\pi}{\omega}\theta\right)$. Accordingly the angular sector without the crack is transformed into the entire plan without the part $X_1 < \mathsf{d_c}(\frac{\ell+d}{\mathsf{d_c}})^{\frac{2\pi}{\omega}}$ of the axis $X_2 = 0$, the cohesive part of the crack being now in the interval $X_1 \in \left(\mathsf{d_c}(\frac{\ell}{\mathsf{d_c}})^{\frac{2\pi}{\omega}}, \mathsf{d_c}(\frac{\ell+d}{\mathsf{d_c}})^{\frac{2\pi}{\omega}}\right)$ of this half line, cf figure 15. The transform changes the distribution of the cohesive forces which are no more uniform but depend on X_1:

$$T(X_1) := \mu \frac{\partial u^i}{\partial X_2}(X_1, 0) = \tau_c \frac{\omega}{2\pi} \left(\frac{X_1}{\mathsf{d_c}}\right)^{\frac{\omega}{2\pi}-1}. \tag{41}$$

Moreover the behaviour at infinity reads now $u^i \sim k\delta_c \sqrt{\frac{R}{\mathsf{d_c}}} \sin \frac{\Theta}{2}$ for large R. Thus, the problem becomes the one of an infinite medium containing a semi infinite crack whose lips are submitted to a given distribution of antiplane forces and whose usual stress intensity factor $\mathsf{K_{III}}$ is known. (With our choice of normalisation of the stress intensity factor, k and $\mathsf{K_{III}}$ are related by $\mathsf{K_{III}} = \mathsf{k}\tau_c\sqrt{\pi \mathsf{d_c}/2}$). Its solution is known and eventually reads as follows:

- The displacement u^i is the real part of an holomorphic function $f(Z)$;
- The stresses are given by the holomorphic function $F(Z) = \mathrm{i}\mu f'(Z)$. Specifically, $\mu\left(\frac{\partial u^i}{\partial X_2} + \mathrm{i}\frac{\partial u^i}{\partial X_1}\right) = F(Z)$;
- F(Z) is given by

$$F(Z) = \frac{\mathsf{k}\tau_c}{2\sqrt{Z/\mathsf{d_c} - b}} + \frac{1}{\pi\sqrt{Z/\mathsf{d_c} - b}} \int_a^b \frac{T(s\mathsf{d_c})\sqrt{b-s}}{s - Z/\mathsf{d_c}} ds \tag{42}$$

with

$$a = \left(\frac{\ell}{\mathsf{d_c}}\right)^{\frac{2\pi}{\omega}}, \qquad b = \left(\frac{\ell+d}{\mathsf{d_c}}\right)^{\frac{2\pi}{\omega}}. \tag{43}$$

It remains to find two relations between the three parameters k, ℓ and d. The first is given by the fact that u^i cannot be singular at the tip of the cohesive zone, because the stress τ_2^i must remains less than τ_c all along the line $x_2 = 0$. The second will be $\ell = 0$ as long as the non-cohesive crack is not appeared. When it is appeared the second relation will be given by the fact that the jump of the displacement at the tip of the non-cohesive crack must be equal to δ_c.

Let us derive the first relation. From (42) $F(Z)$ behaves like $C/\sqrt{Z/\mathsf{d_c} - b}$ in the neighbourhood of the tip of the cohesive zone with C given by

$$C = \frac{\mathsf{k}\tau_c}{2} - \frac{1}{\pi} \int_a^b \frac{T(s\mathsf{d_c})}{\sqrt{b-s}} ds.$$

Hence C must vanish, otherwise the stresses are singular. Using the expression (41) for T gives the desired first relation

$$\mathsf{k} = \frac{\omega}{\pi^2} \int_a^b \frac{s^{\frac{\omega}{2\pi}-1}}{\sqrt{b-s}} ds.$$

Let us set

$$\alpha_m = \arcsin\left(\frac{\ell}{\ell+d}\right)^{\frac{\pi}{\omega}}, \tag{44}$$

α_m characterising the ratio of the non-cohesive crack length over the total crack length. After the change of variable $s = \left(\frac{\ell+d}{\mathsf{d_c}}\right)^{2\pi/\omega} \sin^2 \alpha$ in the integral above, one gets

$$\mathsf{k} = \frac{2\omega}{\pi^2}\left(\frac{\ell+d}{\mathsf{d_c}}\right)^{1-\frac{\pi}{\omega}} \int_{\alpha_m}^{\pi/2} (\sin\alpha)^{\frac{\omega}{\pi}-1} d\alpha. \tag{45}$$

At fix $\ell \geq 0$, the right hand side of (45) is an increasing function of d, growing from 0 to infinity when d grows from 0 to infinity. Hence, for a given $\mathsf{k} > 0$ and a given $\ell \geq 0$, there exists a unique d verifying (45). In other words the size of the cohesive zone is determined by the the length of the non-cohesive crack and the stress intensity factor. In particular, when $\ell = 0$, one gets the following relation between k and d:

$$\mathsf{k} = \frac{2\omega}{\pi^2}\left(\frac{d}{\mathsf{d_c}}\right)^{1-\frac{\pi}{\omega}} \int_0^{\pi/2} (\sin\alpha)^{\frac{\omega}{\pi}-1} d\alpha. \tag{46}$$

Let us now calculate the jump of the displacement at $x_1 = \ell$. Since $\partial u^i/\partial X_2$ is continuous on the lips of the crack and since u^i is skew-symmetric, one gets from the relation between F and f': $\mathrm{i}\mu d[\![u^i]\!]/dX_1 = 2F^+(X_1)$ on the cohesive part of the crack, $F^+(X_1)$ denoting the limit of F when $Z = X_1$ is approached from above. Since $[\![u^i]\!] = 0$ at the tip of the cohesive crack, one deduces the jump of u^i at the tip of the non-cohesive crack by integration. After some calculations not reproduced here, one eventually gets

$$[\![u^i]\!](x_1 = \ell) = \frac{4\omega}{\pi^2}\frac{\ell + d}{\mathsf{d_c}}\delta_c \int_{\alpha_m}^{\pi/2} (\sin\alpha)^{\frac{\omega}{\pi}-1}\left(\cos\alpha_m + \frac{\cos\alpha}{2}\mathrm{Log}\frac{\cos\alpha_m - \cos\alpha}{\cos\alpha_m + \cos\alpha}\right) d\alpha. \tag{47}$$

In (47) it has been taken into account of the relation (45).

When $\ell = 0$, then $\alpha_m = 0$ and the jump of the displacement is proportional to the size of the cohesive zone which itself is a monotonically increasing function of k. Therefore the jump reaches the critical value δ_c and the cohesive crack will appear when k reaches the critical value k_D given by:

$$\mathsf{k}_D = \frac{2\omega}{\pi^2} D^{1-\frac{\pi}{\omega}} \int_0^{\pi/2} (\sin\alpha)^{\frac{\omega}{\pi}-1} d\alpha \tag{48}$$

where D denotes the ratio $d/\mathsf{d_c}$ at this critical loading

$$D = \frac{\pi^2}{4\omega \int_0^{\pi/2} (\sin\alpha)^{\frac{\omega}{\pi}-1}\left(1 + \frac{\cos\alpha}{2}\mathrm{Log}\frac{1-\cos\alpha}{1+\cos\alpha}\right) d\alpha}. \tag{49}$$

After the nucleation of the cohesive crack, *i.e.,* when $\ell > 0$, writing that $[\![u^i]\!](x_1 = \ell) = \delta_c$ in (47) gives $\ell + d$ as a function of α_m. Then using (44) and (45) allows us to obtain also k and ℓ as a function of α_m. That means that the response can be parametrised by α_m with α_m growing from 0. It turns out that k is necessarily decreasing, which means that k_D is a limit load. The onset of the non-cohesive crack is necessarily brutal at k_D.

B. The generic plane strain problem in the neighbourhood of the crack tip for obtaining the fatigue law

The plane is equipped with the cartesian coordinate system (x, y), the associated canonical basis is $(\mathbf{i}, \mathbf{j})$ and $z = x + \mathrm{i}y$ denotes the affixe of the complex number associated with the point (x, y). Let K, L and D be three given real numbers with $\mathsf{K} > 0$ and $\mathsf{D} > 0$. Let us consider the following plane-strain elastic problem whose unknowns are the displacement and stress field $\mathbf{U}$ and $\mathbf{\Sigma}$, cf figure 16:

$$\mathbf{div\Sigma} = 0, \quad \mathbf{\Sigma} = \lambda \mathrm{div}\mathbf{U}\,\mathbf{I} + 2\mu\boldsymbol{\varepsilon}(\mathbf{U}) \quad \text{in} \quad \mathbb{R}^2 \setminus (-\infty, \mathsf{L}+\mathsf{D}) \times \{0\}, \tag{50}$$

$$\Sigma_{12} = \Sigma_{22} = 0 \quad \text{on} \quad (-\infty, \mathsf{L}) \times \{0\}, \qquad \Sigma_{12} = 0, \Sigma_{22} = \sigma_c \quad \text{on} \quad (\mathsf{L}, \mathsf{L}+\mathsf{D}) \times \{0\}, \tag{51}$$

with the condition at infinity

$$\lim_{r\to\infty}\left(\mathbf{U}(x, y) - \frac{\mathsf{K}}{2\mu}\sqrt{\frac{r}{2\pi}}\mathbf{u}^S(\theta)\right) = 0 \tag{52}$$

where $x = r\cos\theta$, $y = r\sin\theta$ and $\mathbf{u}^S(\theta) = (3 - 4\nu - \cos\theta)\left(\cos\frac{\theta}{2}\mathbf{i} + \sin\frac{\theta}{2}\mathbf{j}\right)$.

This problem admits a unique solution which can be obtained in a closed form by using the theory of complex potentials, cf Muskhelishvili (1963). We simply recall here the main results. The fields $\mathbf{U}$ et $\mathbf{\Sigma}$ are related to the function $\varphi(z)$ of the complex variable z by

$$\begin{aligned}
\Sigma_{22}(x, y) - \mathrm{i}\Sigma_{12}(x, y) &= \varphi'(z) + \varphi'(\overline{z}) + (z - \overline{z})\overline{\varphi''(z)}, \\
2\mu\big(U_1(x, y) + \mathrm{i}U_2(x, y)\big) &= (3 - 4\nu)\varphi(z) - \varphi(\overline{z}) - (z - \overline{z})\overline{\varphi'(z)},
\end{aligned}$$

φ being holomorphic in the plane without the half-line $(-\infty, \mathsf{L} + \mathsf{D}) \times \{0\}$, the bar denoting the complex conjugate. By a standard procedure, we get

$$\varphi'(z) = \frac{\sigma_c}{2\pi\sqrt{z - \mathsf{L} - \mathsf{D}}} \int_{\mathsf{L}}^{\mathsf{L}+\mathsf{D}} \frac{\sqrt{\mathsf{L} + \mathsf{D} - x}}{x - z} dx + \frac{\mathsf{K}}{2\sqrt{2\pi(z - \mathsf{L} - \mathsf{D})}}. \tag{53}$$

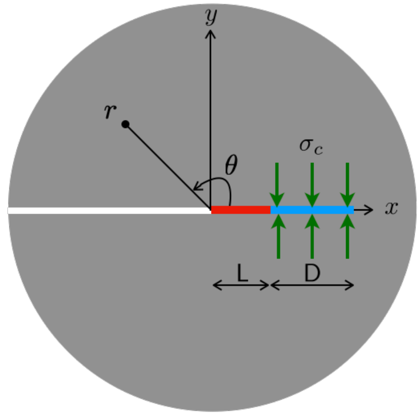

Figure 16: *Data of the generic inner problem, with a behaviour at infinity given by the mode* I *singularity and* K_I *as the stress intensity factor.*

Near the tip $z = \mathsf{L} + \mathsf{D}$, $\varphi'(z)$ behaves like

$$\varphi'(z) \approx \frac{\sqrt{2\pi}\mathsf{K} - 4\sigma_c\sqrt{\mathsf{D}}}{4\pi\sqrt{z - \mathsf{L} - \mathsf{D}}}$$

and hence the stresses are singular with the usual singularity in $1/\sqrt{r}$ except if the factor $\sqrt{2\pi}\mathsf{K} - 4\sigma_c\sqrt{\mathsf{D}}$ vanishes. Specifically, the jump of the normal displacement just behind the tip $x = \mathsf{L} + \mathsf{D}$ and the normal stress just ahead the tip read as

$$[\![U_2]\!](r) = \frac{2(1-\nu^2)}{\pi E}(\sqrt{2\pi}\mathsf{K} - 4\sigma_c\sqrt{\mathsf{D}})\sqrt{r} + \cdots, \qquad \Sigma_{22}(r) = \frac{\sqrt{2\pi}\mathsf{K} - 4\sigma_c\sqrt{\mathsf{D}}}{4\pi\sqrt{r}} + \cdots.$$

Therefore, if it is required that $\Sigma_{22} \le \sigma_c$ on the half-line $(\mathsf{L} + \mathsf{D}, +\infty)\times\{0\}$, then K and D must be such that $\sqrt{2\pi}\mathsf{K} \le 4\sigma_c\sqrt{\mathsf{D}}$. On the other hand, if it is required that $[\![U_2]\!] \ge 0$ holds everywhere (by a non-interpenetration condition, for instance), then K and D must satisfy the converse inequality $\sqrt{2\pi}\mathsf{K} \ge 4\sigma_c\sqrt{\mathsf{D}}$. Accordingly, in order that both conditions are satisfied, the solution must be non singular at the tip $\mathsf{L} + \mathsf{D}$. In such a case D and K are related by

$$\mathsf{K} = 4\sigma_c\sqrt{\frac{\mathsf{D}}{2\pi}}. \tag{54}$$

Assuming from now on that (54) holds, (53) becomes

$$\varphi'(z) = \frac{\sigma_c}{2} + \frac{\mathrm{i}\sigma_c}{2\pi}\left(\mathrm{Log}\left(\sqrt{\mathsf{D}} + \mathrm{i}\sqrt{z - \mathsf{L} - \mathsf{D}}\right) - \mathrm{Log}\left(\sqrt{\mathsf{D}} - \mathrm{i}\sqrt{z - \mathsf{L} - \mathsf{D}}\right)\right). \tag{55}$$

In (55), Log denotes the principal determination of the complex logarithm. After some calculations, one obtains that the normal jump of the displacement along the x-axis reads as

$$[\![U_2]\!](x) = V\left(\frac{x - \mathsf{L}}{\mathsf{D}}\right)\frac{\mathsf{G}}{\mathsf{G_c}}\delta_c \tag{56}$$

where $\mathsf{G_c}$ is the Griffith surface energy density, $\delta_c = \mathsf{G_c}/\sigma_c$ and G denotes the energy release rate which is related to K by Irwin formula, $\mathsf{G} = (1-\nu^2){\mathsf{K_I}}^2/E$. In (56) V denotes the dimensionless real-valued function defined by

$$V(\zeta) = \begin{cases} \sqrt{1-\zeta} - \zeta\ln(1 + \sqrt{1-\zeta}) + \zeta\ln\sqrt{|\zeta|} & \text{if } \zeta \le 1, \zeta \ne 0 \\ 0 & \text{if } \zeta \ge 1 \end{cases} \tag{57}$$

and $V(0) = 1$. Let us note that V is continuously differentiable everywhere (even at $\zeta = 0$ and $\zeta = 1$), is concave for $\zeta \le 0$ and is strictly decreasing from ∞ to 0 when ζ goes from $-\infty$ to 1. When $\zeta \to -\infty$, $V(\zeta) = 2\sqrt{|\zeta|} + o(1)$. The non-interpenetration condition $[\![U_2]\!] \ge 0$ is satisfied everywhere. The normal stress Σ_{22} along the half-line $(\mathsf{L} + \mathsf{D}, +\infty)\times\{0\}$ is given by

$$\Sigma_{22}(x, 0) = \left(1 - \frac{2}{\pi}\arcsin\sqrt{1 - \frac{\mathsf{D}}{x - \mathsf{L}}}\right)\sigma_c. \tag{58}$$

It decreases from σ_c to 0 and, therefore, the condition $\Sigma_{22} \le \sigma_c$ is satisfied.

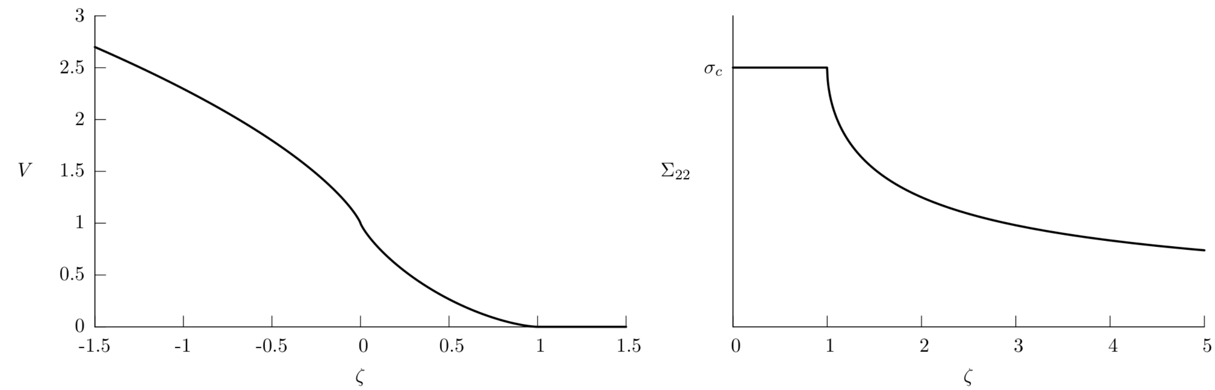

Figure 17: *Graphs of the normal stress and of the function V giving the jump of the normal displacement on the crack path*

References

Abdelmoula, R., Marigo, J.J., Weller, T., 2009b. Construction d'une loi de fatigue à partir d'un modèle de forces cohésives: cas d'une fissure en mode III. Comptes Rendus Mécanique 337, 53 – 59.

Abdelmoula, R., Marigo, J.J., Weller, T., 2010. Construction and justification of Paris-like fatigue laws from Dugdale-type cohesive models. Annals of Solid and Structural Mechanics 1, 139–158.

Abdul-Baqi, A., Schreurs, P.J.G., Geers, M.G.D., 2005. Fatigue damage modeling in solder interconnects using a cohesive zone approach. Int. J. of Sol. and Struct. 42, 927–942.

Amor, H., Marigo, J.J., Maurini, C., 2009. Regularized formulation of the variational brittle fracture with unilateral contact: Numerical experiments. Journal of the Mechanics and Physics of Solids 57, 1209–1229.

Barenblatt, G.I., 1962. The mathematical theory of equilibrium cracks in brittle fracture. Adv. Appl. Mech. 7, 55–129.

Bazant, Z.P., Planas, J., 1998. Fracture and size effect in concrete and other quasibrittle materials. CRC Press.

Bouchitté, G., Braides, A., Buttazzo, G., 1995. Relaxation results for some free discontinuity problems. J. reine angew. Mathematik 458, 1–18.

Bourdin, B., Francfort, G.A., Marigo, J.J., 2008. The variational approach to fracture. Journal of Elasticity 91, 5–148.

Braides, A., Defranceschi, A., Vitali, E., 2001. Relaxation of elastic energies with free discontinuities and constraints on the strain. Ann. Scuola Norm. Sup. Pisa Cl. Sci. 5, 275–317.

Chambolle, A., Francfort, G.A., Marigo, J.J., 2009. When and how do cracks propagate? J. Mech. Phys. Solids 57, 1614–1622.

Charlotte, M., Francfort, G.A., Marigo, J.J., Truskinovky, L., 2000. Revisiting brittle fracture as an energy minimization problem: comparison of Griffith and Barenblatt surface energy models. in: A. Benallal (Eds.), Proceedings of the Symposium on "Continuous Damage and Fracture", in: The Data Science Library, Elsevier, Paris , 7–12.

Charlotte, M., Laverne, J., Marigo, J.J., 2006. Initiation of cracks with cohesive force models: a variational approach. Eur. J. Mech. A-Solid 25, 649–669.

Conti, S., Focardi, M., Iurlano, F., 2016. Phase field approximation of cohesive fracture models. Annales de l'Institut Henri Poincaré C, Analyse non linéaire 33, 1033–1067.

Dal Maso, G., Garroni, A., 2008. Gradient bounds for minimizers of free discontinuity problems related to cohesive zone models in fracture mechanics. Calculus of Variations and Partial Differential Equations 31, 137–145.

Del Piero, G., 1999. One-dimensional ductile-brittle transition, yielding and structured deformations. in: P. Argoul, M. Frémond (Eds.), Proceedings of IUTAM Symposium "Variations de domaines et frontières libres en mécanique", Paris, 1997, Kluwer Academic .

Dugdale, D.S., 1960. Yielding of steel sheets containing slits. J. Mech. Phys. Solids 8, 100–108.

Griffith, A., 1921. The phenomena of rupture and flow in solids. Phil. Trans. Roy. Soc. London CCXXI, 163–198.

Maiti, S., Geubelle, P., 2005. A cohesive model for fatigue failure of polymers. Eng. Fract. Mech. 72, 691–708.

Mielke, A., 2005. Evolution of rate-independent systems, in: Evolutionary equations. Elsevier/North-Holland, Amsterdam. volume II of *Handb. Differ. Equ.*, pp. 461–559.

Muskhelishvili, N.I., 1963. Some basic problems of mathematical theory of elasticity. P. Noordhoff Ltd, Groningen.

Nguyen, O., Repetto, E.A., Ortiz, M., Radovitzki, R.A., 2001. A cohesive model of fatigue crack growth. Int. J. of Fract. 110, 351–369.

Paris, P.C., Erdogan, F., 1963. A critical analysis of crack propagation laws. Journal of Basic Engineering 85, 528–534.

Paris, P.C., Gomez, M.P., Anderson, W.E., 1961. A rational analytic theory of fatigue. The Trend in Engineering 13, 9–14.

Roe, K.L., Siegmund, T., 2002. An irreversible cohesive zone model for interface fatigue crack growth simulation. Eng. Fract. Mech. 70, 209–232.

Siegmund, T., 2004. A numerical study of transient fatigue crack growth by use of an irreversible cohesive zone model. Int. J. of Fatigue 26, 929–939.

Talon, C., Curnier, A., 2003. A model of adhesion coupled to contact and friction. European Journal of Mechanics A/Solids 22.

Yang, B., Mall, S., Ravi-Chandar, K., 1999. A cohesive zone model for fatigue crack growth in quasibrittle materials. Int. J. of Sol. and Struct. 38, 3927–3944.